

Fourfold path to Thermality: Inequivalent purifications of Rindler wedge

Rakesh k Jha*

Department of Physics,
Birla Institute of Technology and Science,
Pilani-Hyderabad Campus
Hyderabad, 500078, India
(Dated: January 30, 2026)

We investigate thermal behaviour in quantum fields by analysing a hierarchy of null-shifted Rindler wedges in Minkowski spacetime. Starting from the Minkowski vacuum restricted to an initial Rindler wedge, we construct several inequivalent transformation paths, including direct Minkowski-to-Rindler mappings, spatial translations, and sequential null displacements, and study the resulting particle content using Bogoliubov transformations. In the standard Unruh effect, horizon-induced entanglement between left- and right-moving sectors gives rise to Gibbsian thermality, with both sectors exhibiting thermal occupation numbers described by a mixed Gibbs state. In contrast, we show that null-shifted wedge constructions lead to a selective and non-Gibbsian form of thermality, in which only a single chiral sector develops Bose–Einstein–distributed occupation numbers. At the same time, the complementary sector remains in a vacuum. Along composite transformation paths, the global Minkowski state remains pure, and the induced states associated with null-shifted wedges are themselves pure tensor-product states. The resulting thermal behaviour arises from Bogoliubov mixing and modular time evolution rather than from entanglement across a horizon or the emergence of a Gibbs density matrix. These findings demonstrate the existence of inequivalent purifications of thermal occupation spectra and clarify the distinct roles of horizon structure, observer dependence, Bogoliubov transformations, and entanglement in the emergence of thermality. In this sense, the null-shifted construction may be viewed as a converse of the Unruh effect, wherein thermal behaviour arises without entanglement-induced mixedness. Our results establish that the appearance of thermal spectra in Rindler wedges does not uniquely imply Gibbsian thermality or horizon-induced entanglement, highlighting the operational independence of thermality and entanglement in relativistic quantum field theory.

Keywords: Unruh effect; Rindler spacetime; Bogoliubov transformations; Selective thermalization; Quantum field theory in curved spacetime; Inequivalent purifications of vacuum

I. INTRODUCTION

The Unruh effect reveals a deep interplay between quantum field theory, spacetime structure, and thermality. A uniformly accelerated observer in Minkowski spacetime perceives the inertial vacuum as a thermal state, with a temperature proportional to the proper acceleration. In the Rindler description, this phenomenon is understood as a consequence of horizon-induced entanglement; the Minkowski vacuum is entangled between causally disconnected Rindler wedges, and restricting the global vacuum state to a single wedge yields a mixed thermal density matrix[1]. From the perspective of algebraic quantum field theory, this thermality arises because the local algebra associated with a Rindler wedge possesses a nontrivial commutant[2], and the reduced state is obtained by tracing over the complementary algebra. An astrophysical black hole is predicted to radiate thermal Hawking radiation with a temperature roughly proportional to the inverse of the black hole mass [3]. The Rindler spacetime offers a simpler setting where black hole radiation can be studied and understood.

While the Unruh effect is traditionally formulated

in this setting, it is natural to pose a converse question: given a Rindler wedge in which an accelerated observer detects a thermal spectrum, what are the possible global states and spacetime regions that can give rise to such thermality upon restriction to that wedge? The Minkowski vacuum provides a canonical realisation of this phenomenon, but it is not evident that it is unique. Addressing this converse problem allows us to investigate whether thermality in Rindler spacetime must necessarily originate from entanglement across horizons, or whether alternative mechanisms can produce thermal spectra in accelerated frames. In this work, by a thermal spectrum we mean the characteristic occupation-number distribution detected by an accelerated observer, without assuming that the underlying state is a Gibbs thermal density matrix.

In this work, we explore this question by systematically comparing two classes of transformations relating different Rindler wedges, spatial shifts and null shifts. We focus on the wedge R_3 , which serves as the observer’s accessible region. In the case of spatial shifts, the transformation preserves the causal structure in a manner closely analogous to the standard Rindler decomposition. The resulting state in R_3 exhibits thermal behaviour that can still be traced to entanglement between causally separated regions, and the associated reduced state remains mixed. In this sense, spatial shifts retain the essential

* jhark007.qg@gmail.com

structural features of the Unruh effect.

The situation changes qualitatively in the presence of null shifts. A null shift corresponds to a translation along a horizon generator and, unlike the standard Rindler partition, does not introduce a new causally inaccessible region. Instead, null shifts preserve causal accessibility along the horizon generators and therefore do not lead to a decomposition of the Hilbert space into complementary algebras. As a result, the algebra associated with a null-shifted wedge does not admit a nontrivial commutant that would play the role of an inaccessible region[2, 4]. No tracing over external degrees of freedom is performed, and the global state remains pure when restricted to the null-shifted wedges R_2 , R_4 , and R_3 . Nevertheless, the Bogoliubov transformation relating the corresponding mode decompositions gives rise to a thermal particle spectrum as detected by an accelerated observer. In particular, the states in R_2 and R_4 naturally correspond to outgoing and ingoing modes, respectively, while the state in R_3 is related to them by a null translation of the corresponding mode decomposition.

This demonstrates that the thermality observed in null-shifted wedges is not of the Unruh type. In the standard Unruh effect, thermality is inseparably tied to horizon-induced entanglement and the resulting thermofield-double structure obtained by tracing over causally inaccessible degrees of freedom. By contrast, the null-shift construction yields thermal particle spectra within globally pure states and without entanglement between distinct wedges. In this precise sense, null shifts realise a converse (in the sense of reversing the logical origin of thermality) to the Unruh effect; rather than thermality emerging from tracing over entangled degrees of freedom, it arises from kinematical Bogoliubov mixing induced by horizon-preserving translations.

We show that the converse problem admits multiple inequivalent realisations, corresponding to distinct embeddings of observer-detected thermal spectra in Rindler spacetime. By contrasting spatial and null shifts, we uncover a richer structure underlying thermality in accelerated frames and demonstrate that thermal spectra in Rindler wedges do not uniquely characterise the Unruh effect. Our results highlight that thermality in quantum field theory can arise through mechanisms fundamentally different from horizon-induced entanglement, thereby broadening the conceptual landscape of the Unruh phenomenon.

We consider a massless scalar field defined on two-dimensional Minkowski spacetime and investigate the emergence of thermality in a fixed Rindler wedge R_3 . All quantum states are taken to be globally defined on Minkowski spacetime, and the physical properties observed in R_3 arise from restricting these global states to the algebra of observables associated with the wedge.

Path 1 corresponds to the standard Unruh setup, in which the global state is the Minkowski vacuum $|0_M\rangle$. When restricted to the Rindler wedge R_3 , this state yields a reduced density matrix that is thermal with respect to

the boost generator associated with R_3 , reproducing the usual Unruh effect.

In Path 2, we consider a larger Rindler wedge R_1 such that $R_3 \subset R_1$, with the bifurcation points of R_1 and R_3 separated by a spacelike interval. The global state is chosen so that its restriction to R_1 coincides with the Rindler vacuum associated with R_1 . This state is not Hadamard when viewed as a state on Minkowski spacetime and exhibits singular behaviour on the Rindler horizon. Nevertheless, we analyse its restriction to R_3 as a useful comparison case, illustrating how thermodynamic properties in R_3 depend on the choice of global vacuum.

Paths 3 and 4 are constructed in closer analogy with black hole physics. We consider null-shifted Rindler wedges R_2 and R_4 , both of which contain R_3 , and global quantum states characterised by nontrivial energy fluxes along null directions. In Path 3, the global state carries an outward flux of scalar particles, analogous to outgoing radiation in the near-horizon region of a collapsing spacetime. In Path 4, the global state is characterised by an inward thermal flux of scalar particles, analogous to ingoing thermal radiation outside a black hole horizon. In both cases, the properties observed in R_3 arise from restricting these globally defined flux-carrying states to the wedge R_3 .

We also show an interesting effect; we consider a Rindler wedge with either an outgoing or an ingoing particle flux and convert it to a particle density in a Rindler wedge that is a subset of the previous wedge. The paths three and four in the previous paragraph use this effect to determine the particle density.

We mention a few caveats and assumptions followed in this work. The analysis is done using two methods. One is via mode functions and explicitly evaluating the Bogoliubov coefficients. The other method is using the Virasoro anomaly in two-dimensional conformal field theory (2d CFT). Since in this article we consider a massless scalar field in two dimensions, the techniques of 2d conformal field theory are applicable. We use the well known Virosoro anomaly to evaluate the stress tensor to prove the particle content in various Rindler wedges. In the analysis done in this article, we assume that the magnitude of acceleration is large and the calculations are valid close to the horizon of the uniformly accelerating observer.

As mentioned earlier, the starting point of Path 2 is Rindler spacetime with a scalar field in the Rindler vacuum. When viewed as a state on Minkowski spacetime, the Rindler vacuum is not Hadamard and exhibits a divergent local stress tensor on the Rindler horizon. As discussed in the literature [5], the Boulware vacuum in black hole spacetimes exhibits analogous near-horizon behaviour, although it is globally distinct and defined in curved spacetime. We include Path 2 as a diagnostic example rather than a physically realisable state. It is important to emphasise that the thermality encountered in null-shifted wedges is non-Gibbsian in nature, although thermal particle spectra arise, the corresponding states

| Scenario | What changes? | What the observer sees in R_3 | State nature | Entanglement? | Type of thermality |
|-------------------------|---------------------------------|-------------------------------------|--------------|---------------|-------------------------------|
| Unruh effect | Accelerated observer | Thermal spectrum in both sectors | Mixed state | Yes | Gibbsian (true thermal state) |
| Spatial shift of wedges | Spatial displacement of horizon | Thermal spectrum in both sectors | Mixed state | Yes | Gibbsian (Unruh-type) |
| Null shift of wedges | Translation along the horizon | Thermal spectrum in one sector only | Pure state | No | Non-Gibbsian (selective) |

TABLE I. Physical interpretation of thermality in different Rindler constructions. The Unruh effect and spatial shifts yield genuine Gibbsian thermality associated with entanglement across horizons. In contrast, null-shifted wedges exhibit selective, non-Gibbsian thermal behaviour, where thermal particle spectra emerge without entanglement and the underlying quantum states remain pure.

are not thermal density matrices of the form $\rho \propto e^{-\beta H}$, but remain globally and locally pure.

To clarify the conceptual distinctions between the different mechanisms of thermality studied in this work, we summarise their key features in Table I. In particular, the table highlights the contrast between Gibbsian thermality arising from horizon-induced entanglement and the non-Gibbsian thermal behaviour generated by null-shifted Bogoliubov transformations.

The remainder of this paper is organised as follows. In Section II, we review the quantisation of a massless scalar field in two-dimensional Minkowski spacetime and introduce the relevant Rindler wedges, mode decompositions, and vacuum states that form the basis of our analysis. In Section III, we present the two complementary methods used throughout the paper to diagnose thermality: an explicit Bogoliubov transformation analysis of mode functions, and an independent computation of the stress tensor using the Virasoro anomaly in two-dimensional conformal field theory.

Section IV constitutes the core of the paper, where we investigate the particle content observed in a fixed Rindler wedge R_3 along four distinct paths. Path 1 reproduces the standard Unruh effect by restricting the Minkowski vacuum to R_3 . Path 2 considers a global state that coincides with the Rindler vacuum in a larger wedge and illustrates how non-Hadamard behaviour leads to inequivalent thermodynamic properties upon restriction. Paths 3 and 4 involve null-shifted Rindler wedges and global states carrying outgoing or ingoing fluxes, respectively, and demonstrate how thermal particle spectra can arise in R_3 within globally pure states through kinematical Bogoliubov mixing.

In Section V, we compare the stress tensor expectation values obtained along different paths and show that, while particle spectra may appear thermal in all cases, the underlying states are physically inequivalent. Finally, in Section VI, we discuss the broader implications of our results for the interpretation of horizon thermality, clarify the sense in which null-shift constructions realise a converse to the Unruh effect, and comment on possible connections to black hole physics.

II. THE PROBLEM STATEMENT AND SETUP

We consider a fixed Rindler wedge R_3 and a massless real scalar field defined globally on two-dimensional Minkowski spacetime. We aim to investigate how thermal particle spectra observed in R_3 can arise from restricting globally defined quantum states to the algebra of observables associated with R_3 . In particular, we ask whether the global spacetime region and quantum state leading to a given particle content in R_3 are uniquely determined. As outlined in the Introduction, we show that this is not the case; distinct choices of global states and spacetime regions, related by spatial or null shifts of Rindler wedges, can lead to identical or similar thermal spectra when restricted to R_3 . To address this question systematically, we introduce below several distinct paths corresponding to different sequences of wedge restrictions and coordinate transformations.

A. Four inequivalent paths

We discuss below the various paths leading to a common end point viz wedge R_3 having a thermal distribution of particles in the high acceleration regime (close to the horizons). As stated before in the introduction, we show that various starting points yield the common endpoint. By starting points, we mean various spacetimes with the massless scalar fields in corresponding particle states. We demonstrate this by explicitly choosing the starting points and evaluating the final particle content in R_3 along the given path.

1. Path 1: Minkowski (in vacuum state) M to Rindler wedge R_3

In this path, we consider Minkowski spacetime with the massless scalar field in a vacuum state. The wedge R_3 is located such that its bifurcation point is situated to the right of the origin. The Unruh effect states that the reduced state of the massless scalar field in R_3 is a thermal distribution of particles.

2. Path 2: Rindler wedge R_1 in vacuum state to Rindler wedge R_3 via Spatial Shift

In Path 2, the wedge R_3 is defined from R_1 by a spatial translation, characterised by displacement parameter Δ_1 (cf. Figure 1). Although the bifurcation point of R_3 is shown along the x_1 axis, its precise location may be generalised to any point within the (u, v) light-cone plane.

3. Path 3: Sequential Null Shifts

Path 3 traces a sequence $R_1 \rightarrow R_2 \rightarrow R_3$, where

R_2 is obtained from R_1 by displacing its origin along the future-directed null V_1 -axis by a Minkowski parameter Δ_2 , R_3 is then constructed by a further displacement of R_2 along the null U_2 -axis by parameter Δ_3 (see Figure 1). For illustration, Figure 1 depicts the case where $\Delta_2 = \Delta_3$, but this equality is not a physical constraint and can be ensured by an appropriate Lorentz transformation, since these parameters are not Lorentz scalars.

4. Path 4: Null Shifts via Rindler Wedge R_4

Path 4 involves the wedge R_4 , whose origin is obtained from R_1 by a null shift along the U_1 -axis by parameter Δ_4 . Subsequently, R_3 is reached by an additional null shift from R_4 along the V_2 -axis with parameter Δ_3 , as depicted in Figure 2. The wedge R_4 is an independent Rindler wedge analogous to R_2 , obtained by shifting through a different null axis, and plays a central role in the construction of this path.

These construction paths serve to systematically characterise inequivalent purifications of Rindler vacua and reveal how selective and full thermalisation arise in distinct regions of spacetime. While intermediate wedges are omitted in some scenarios for simplicity, the analysis extends to more general initial states, though with potentially differing particle spectra [6].

B. Coordinate Relations among the key players

Two dimensional Minkowski spacetime is denoted as M , parametrized by inertial coordinates (X, T) , and a hierarchy of Rindler wedges [7], denoted (R_i) , each described by coordinates (x_i, t_i) for $i \in \{1, 2, 3, 4\}$. As depicted in Figs. 1 and 2, the nested structure of Rindler wedges are understood as inclusions of spacetime regions determined by their null horizons, such that $R_3 \subset R_2 \subset R_1 \subset M$, and $R_3 \subset R_4 \subset R_1 \subset M$, with individual wedges distinguished by the shaded regions in pale red, blue, and green. Wedges R_2 and R_3 are generated from R_1 by successive null displacements along the relevant Minkowski light rays, a construction central to our analysis.

1. Various Rindler wedges and their coordinate relationships

We label the coordinates of the Rindler-1 (R_1) frame as (x_1, t_1) . The transformation between the Rindler-1 coordinates (R_1) and Minkowski (M) is given by:

$$T = \frac{e^{a_1 x_1}}{a_1} \sinh(a_1 t_1), \quad (1)$$

$$X = \frac{e^{a_1 x_1}}{a_1} \cosh(a_1 t_1), \quad (2)$$

we now introduce the light-cone coordinates in R_1 , (u_1, v_1) :

$$u_1 = t_1 - x_1, \quad v_1 = t_1 + x_1,$$

And the lightcone coordinates in Minkowski spacetime are related to the coordinates of R_1 as:

$$U_M = T - X = -\frac{e^{-a_1 u_1}}{a_1}, \quad (3)$$

$$V_M = T + X = \frac{e^{a_1 v_1}}{a_1}, \quad (4)$$

2. Minkowski to Rindler-3 and Rindler 1 to Rindler-3 via spatial shift along x_1 axis

We label the coordinates of the Rindler-3 (R_3) as (x_3, t_3) . In the setup, we already mentioned that we do not assume any intermediate wedges between R_1 and R_3 . We now relate Rindler-3 (R_3) to Minkowski space. Its transformation is given by:

$$T = \frac{e^{a_3 x_3}}{a_3} \sinh(a_3 t_3), \quad (5)$$

$$X = \frac{e^{a_3 x_3}}{a_3} \cosh(a_3 t_3) + \Delta_1. \quad (6)$$

where Δ_1 encodes the coordinate shift in the Rindler space, along x_1 axis relates the wedge R_3 to R_1 . And the lightcone coordinates in Minkowski spacetime are related to the coordinates of R_3 as:

$$U_M = T - X = -\frac{e^{-a_3 u_3}}{a_3} - \Delta_1, \quad (7)$$

$$V_M = T + X = \frac{e^{a_3 v_3}}{a_3} + \Delta_1, \quad (8)$$

In a given Rindler frame, the parameter that represents acceleration is a_1 for the wedge R_1 . We note that if we choose an alternative parameter b_1 as the acceleration parameter, we obtain a different coordinate system for the same wedge. One can set up the description of the quantum field in the new coordinate system. It is easy to prove that both descriptions share the vacuum state, as the Bogoliubov coefficients between the modes defined in either coordinate system mix only positive-frequency modes of one coordinate system with the positive-frequency modes of the other coordinate system. Therefore, we are free to choose whichever parameter we want in a given Rindler wedge. This choice amounts to selecting a particular accelerating observer from among a family of accelerating observers that accelerate at different proper accelerations, all of which share the same horizon. Therefore, we set $a_1 = a_2 = a_3 = a$, which simplifies the calculation without losing generality. Equating Eq. (3) and Eq. (7), we have;

$$u_1 = -\frac{1}{a} \ln(e^{-a u_3} + a \Delta_1), \quad (9)$$

Also from Eq. (4) and Eq. (8), we have;

$$v_1 = \frac{1}{a} \ln(e^a v_3 + a \Delta_1), \quad (10)$$

From Eq. (9) and Eq. (10) and at $\Delta_1 = \frac{1}{a}$ we obtain,

$$u_1 = -\frac{1}{a} \ln(e^{-a} u_3 + 1), \quad (11)$$

$$v_1 = \frac{1}{a} \ln(e^a v_3 + 1). \quad (12)$$

3. Rindler 1 to Rindler 3 via Rindler 2: series of null shifts

We label the coordinates of the Rindler-1 (R_1) frame as (x_1, t_1) , Rindler-2 (R_2) as (x_2, t_2) , and Rindler-3 (R_3) as (x_3, t_3) .

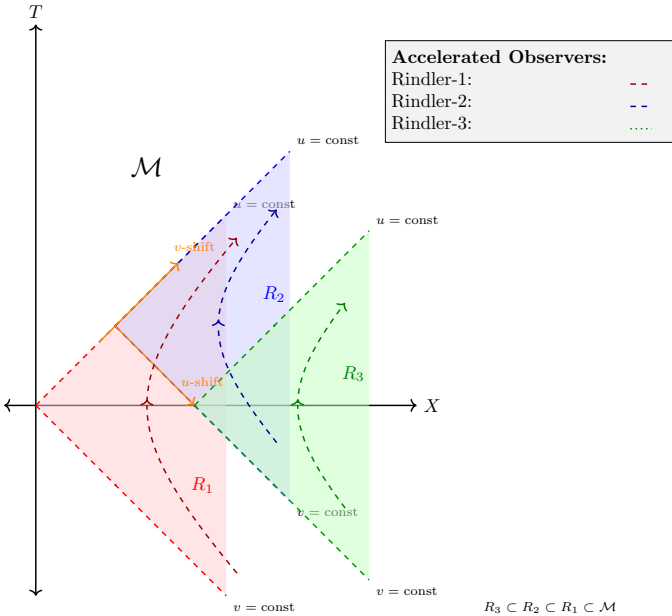


FIG. 1. Null-shifted Rindler wedges in Minkowski spacetime. The standard right Rindler wedge is successively shifted along the future-directed null V -direction to obtain (R_2) and then along the U -direction to obtain (R_3).

The frame R_2 is null shifted along the V_1 axis. Its coordinates relate to Minkowski as follows:

$$T = \frac{e^{a x_2}}{a} \sinh(a t_2) + \Delta_2, \quad (13)$$

$$X = \frac{e^{a x_2}}{a} \cosh(a t_2) + \Delta_2. \quad (14)$$

Where Δ_2 encodes the coordinate shift in the Rindler space that relates the wedge R_2 to R_1 . The lightcone coordinates of Minkowski spacetime and those of R_2 are

related by:

$$U_M = T - X = -\frac{e^{-a} u_2}{a}, \quad (15)$$

$$V_M = T + X = \frac{e^a v_2}{a} + 2 \Delta_2. \quad (16)$$

Equating Eq. (3) and Eq. (15), we have;

$$u_1 = u_2, \quad (17)$$

Also from Eq. (4) and Eq. (16), at $\Delta_2 = 1/2a$ we have;

$$v_1 = \frac{\ln(e^a v_2 + 1)}{a}, \quad (18)$$

We now relate Rindler-3 (R_3) to Minkowski space. Its transformation is given by:

$$T = \frac{e^{a x_3}}{a} \sinh(a t_3) + (\Delta_2 - \Delta_3), \quad (19)$$

$$X = \frac{e^{a x_3}}{a} \cosh(a t_3) + (\Delta_2 + \Delta_3). \quad (20)$$

where Δ_3 encodes the coordinate shift in the Rindler space that relates the wedge R_3 to R_2 . In light-cone form:

$$U_M = T - X = -\frac{e^{-a} u_3}{a} - 2 \Delta_3, \quad (21)$$

$$V_M = T + X = \frac{e^a v_3}{a} + 2 \Delta_2. \quad (22)$$

Matching with the coordinates of R_2 , at $\Delta_2 = 1/2a$ we find:

$$u_2 = -\frac{\ln[e^{-a} u_3 + 1]}{a}, \quad (23)$$

$$v_2 = v_3. \quad (24)$$

Without loss of generality, we choose $\Delta_3 = \Delta_2$. This is because we can choose a suitable Lorentz transformation in which both the parameters are equal, and hence the bifurcation point of R_3 lies on the x_1 axis, simplifying the geometry without altering the physical content.

4. Rindler 1 to Rindler 3 via Rindler 4: series of null shifts

Analogously, consider null shifts along the U -axis, as shown in Fig. 2

The frame R_1 remains as:

$$T = \frac{e^{a x_1}}{a} \sinh(a t_1), \quad (25)$$

$$X = \frac{e^{a x_1}}{a} \cosh(a t_1). \quad (26)$$

In light-cone form:

$$U_M = -\frac{e^{-a} u_1}{a}, \quad (27)$$

$$V_M = \frac{e^a v_1}{a}. \quad (28)$$

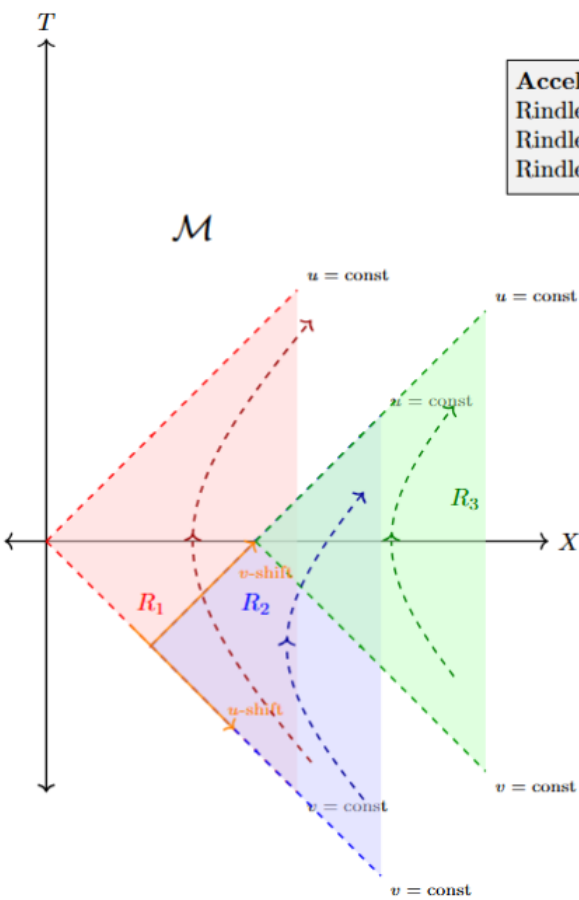


FIG. 2. Alternative null-shift construction. The wedge (R_4) is obtained from (R_1) by a null shift along the U -direction, followed by a shift along the V -direction to obtain (R_3). As in Fig. 1, the construction results in nested spacetime regions.

Now consider R_4 , shifted along the U -axis.

$$T = \frac{e^{a x_4}}{a} \sinh(a t_4) - \Delta_4, \quad (29)$$

$$X = \frac{e^{a x_4}}{a} \cosh(a t_4) + \Delta_4. \quad (30)$$

In light-cone form:

$$U_M = -\frac{e^{-a u_4}}{a} - 2 \Delta_4, \quad (31)$$

$$V_M = \frac{e^{a v_4}}{a}. \quad (32)$$

From Eq. (27) and Eq. (31), at $\Delta_4 = 1/2a$ we obtain:

$$u_1 = -\frac{\ln(e^{-a u_4} + 1)}{a}, \quad (33)$$

and from Eq. (28) and Eq. (32):

$$v_1 = v_4, \quad (34)$$

Finally, for R_3 :

$$\boxed{\text{Accelerated Observers: } T = \frac{e^{a x_3}}{a} \sinh(a t_3) - (\Delta_4 - \Delta_3), \quad (35)}$$

$$\boxed{\text{Rindler-1: } X = \frac{e^{a x_3}}{a} \cosh(a t_3) + (\Delta_4 + \Delta_3). \quad (36)}$$

In light-cone form:

$$U_M = -\frac{e^{-a u_3}}{a} - 2 \Delta_4, \quad (37)$$

$$V_M = \frac{e^{a v_3}}{a} + 2 \Delta_3. \quad (38)$$

Matching the coordinates of R_4 , and also without loss of generality, we choose $\Delta_4 = \Delta_3 = \frac{1}{2a}$. We then obtain the following.

$$u_4 = u_3, \quad (39)$$

$$v_4 = \frac{1}{a} \ln(e^{a v_3} + 1). \quad (40)$$

These expressions completely characterise the relationships among the Rindler patches that shift to the null in the U and V directions.

These construction paths serve to systematically characterise inequivalent purifications of Rindler vacua and reveal how selective and full thermalisation arise in distinct regions of spacetime. While intermediate wedges are omitted in some scenarios for simplicity, the analysis $R_3 \subset R_2 \subset R_1 \subset M$ extends to more general initial states, though with potentially differing particle spectra [6].

Having established the coordinate relations among the Rindler wedges and the four inequivalent paths leading to R_3 , we now turn to the operational question: what does an observer in R_3 actually measure along each path? In particular, we diagnose thermality using two complementary criteria, (i) the expectation value of particle number operators defined with respect to R_3 modes, and (ii) the expectation value of the stress tensor computed via the Virasoro anomaly. These diagnostics allow us to distinguish Gibbsian thermality arising from entanglement from non-Gibbsian thermality arising purely from Bogoliubov mixing.

III. METHODOLOGY

In the previous section, we defined the coordinate systems in various spacetimes relevant to the problem and then obtained the relations between them. To determine the particle content in various spacetimes, we use two techniques. One is the canonical way to set up the mode expansion of scalar fields and evaluate the Bogoliubov coefficient. Another useful method is using the Virasoro anomaly.

A. Bogoliubov method

We begin by considering a free, massless scalar field in $(1+1)$ -dimensional Rindler spacetime. The field satisfies

the Klein–Gordon equation,

$$\square \hat{\phi}(x^\mu) = 0, \quad (41)$$

where $\square = \eta^{\mu\nu} \nabla_\mu \nabla_\nu$.

In conformally flat form, the Rindler metric allows Eq. (41) to be rewritten as

$$e^{2ax} \square \hat{\phi}(x^\mu) = \left(\frac{\partial^2}{\partial t^2} - \frac{\partial^2}{\partial x^2} \right) \hat{\phi}(x^\mu) = 0. \quad (42)$$

In $(1+1)$ dimensions, the general solution separates into right-moving and left-moving modes, propagating along the null coordinates $u = t - x$, $v = t + x$. Accordingly, the quantum scalar field operator in a single Rindler wedge R_i can be expanded as [8]

$$\begin{aligned} \hat{\phi}(x_i, t_i) = \int_0^\infty d\omega & \left[\vec{a}_i(\omega) f_i(\omega) + \vec{a}_i^\dagger(\omega) f_i^*(\omega) \right. \\ & \left. + \hat{b}_i(\omega) g_i(\omega) + \hat{b}_i^\dagger(\omega) g_i^*(\omega) \right], \end{aligned} \quad (43)$$

where $\vec{a}_i(\omega)$ and $\hat{b}_i(\omega)$ are the annihilation operators associated with right- and left-moving modes, respectively. The mode functions take the form

$$f_i(\omega) = N_\omega e^{-i\omega(t-x)}, \quad g_i(\omega) = N_\omega e^{-i\omega(t+x)}.$$

The normalisation constant N_ω is determined by requiring orthonormality of the modes under the Klein–Gordon inner product, defined on a constant-time hypersurface Σ as [9]

$$\langle \phi_1, \phi_2 \rangle = i \int_\Sigma d^{n-1}\Sigma \sqrt{\gamma} \eta^\mu (\phi_1^* \nabla_\mu \phi_2 - \phi_2 \nabla_\mu \phi_1^*). \quad (44)$$

For right- and left-moving modes, this reduces to [10]

$$\langle f_l, f_m \rangle = -i \int_\Sigma du (f_l \partial_u f_m^* - f_m^* \partial_u f_l), \quad (45)$$

$$\langle g_l, g_m \rangle = -i \int_\Sigma dv (g_l \partial_v g_m^* - g_m^* \partial_v g_l), \quad (46)$$

for $l \neq m = 1, 2$. From this normalisation condition, one obtains

$$N_\omega = \frac{1}{\sqrt{4\pi\omega}}. \quad (47)$$

It follows that the full scalar field operator splits into independent right- and left-moving sectors,

$$\hat{\phi}(x) = \hat{\phi}(u) + \hat{\phi}(v).$$

We now introduce the mode expansions of the scalar field in the various Rindler wedges relevant to our analysis. These modes represent the natural positive-frequency excitations with respect to the proper time of uniformly accelerated observers associated with each wedge. Since thermality in Rindler spacetime is defined

operationally through the response of such observers, particle content must be evaluated by comparing these mode decompositions across different wedges. Although several Rindler frames are introduced below, in each path, only a specific subset of modes undergoes nontrivial Bogoliubov mixing. Crucially, in two dimensions the field separates into independent right- and left-moving sectors, allowing us to track how thermal behaviour may arise in one chiral sector while the other remains in its vacuum. This chiral structure will play a central role in distinguishing full Gibbsian thermality from the selective, non-Gibbsian thermality induced by null shifts. The right-moving component in wedge R_1 takes the form

$$\hat{\phi}_1(u_1) = \int_0^\infty \frac{d\omega}{\sqrt{4\pi\omega}} \left[\vec{a}_1(\omega) e^{-i\omega u_1} + \vec{a}_1^\dagger(\omega) e^{i\omega u_1} \right], \quad (48)$$

while in the remaining wedges the expansions are

$$\hat{\phi}_2(u_2) = \int_0^\infty \frac{d\Omega}{\sqrt{4\pi\Omega}} \left[\vec{a}_2(\Omega) e^{-i\Omega u_2} + \vec{a}_2^\dagger(\Omega) e^{i\Omega u_2} \right], \quad (49)$$

$$\hat{\phi}_3(u_3) = \int_0^\infty \frac{d\nu}{\sqrt{4\pi\nu}} \left[\vec{a}_3(\nu) e^{-i\nu u_3} + \vec{a}_3^\dagger(\nu) e^{i\nu u_3} \right], \quad (50)$$

$$\hat{\phi}_4(u_4) = \int_0^\infty \frac{d\rho}{\sqrt{4\pi\rho}} \left[\vec{a}_4(\rho) e^{-i\rho u_4} + \vec{a}_4^\dagger(\rho) e^{i\rho u_4} \right]. \quad (51)$$

Analogously, the left-moving components of the field operator are

$$\hat{\phi}_1(v_1) = \int_0^\infty \frac{d\omega}{\sqrt{4\pi\omega}} \left[\hat{b}_1(\omega) e^{-i\omega v_1} + \hat{b}_1^\dagger(\omega) e^{i\omega v_1} \right], \quad (52)$$

$$\hat{\phi}_2(v_2) = \int_0^\infty \frac{d\Omega}{\sqrt{4\pi\Omega}} \left[\hat{b}_2(\Omega) e^{-i\Omega v_2} + \hat{b}_2^\dagger(\Omega) e^{i\Omega v_2} \right], \quad (53)$$

$$\hat{\phi}_3(v_3) = \int_0^\infty \frac{d\nu}{\sqrt{4\pi\nu}} \left[\hat{b}_3(\nu) e^{-i\nu v_3} + \hat{b}_3^\dagger(\nu) e^{i\nu v_3} \right], \quad (54)$$

$$\hat{\phi}_4(v_4) = \int_0^\infty \frac{d\rho}{\sqrt{4\pi\rho}} \left[\hat{b}_4(\rho) e^{-i\rho v_4} + \hat{b}_4^\dagger(\rho) e^{i\rho v_4} \right]. \quad (55)$$

Here, the frequency parameters ω, Ω, ν , and ρ denote the mode labels associated with wedges R_1, R_2, R_3 , and R_4 , respectively.

B. Bogoliubov Transformation and the Number Operator

In this section, we derive the Bogoliubov transformation relating two complete sets of mode functions and use it to compute the expectation value of the number operator in different Rindler frames.

Let $\{f_i(\omega)\}$ and $\{f_j(\Omega)\}$ denote two complete sets of positive-norm, orthonormal mode functions with respect to the Klein–Gordon inner product defined in Eq. (44). These mode sets are related by the Bogoliubov transformation [11, 12]:

$$f_j(\Omega) = \int_{-\infty}^{\infty} d\omega [\alpha_{ji}(\Omega, \omega) f_i(\omega) + \beta_{ji}(\Omega, \omega) f_i^*(\omega)], \quad (56)$$

and conversely,

$$f_i(\omega) = \int_{-\infty}^{\infty} d\Omega [\alpha_{ji}^*(\Omega, \omega) f_j(\Omega) - \beta_{ji}(\Omega, \omega) f_j^*(\Omega)]. \quad (57)$$

Here, α_{ji} and β_{ji} are the Bogoliubov coefficients encoding the mixing of positive- and negative-frequency modes between the two bases.

A real scalar quantum field $\hat{\Phi}$ can be expanded in either basis as

$$\hat{\Phi} = \int_{-\infty}^{\infty} d\omega [\hat{a}_i(\omega) f_i(\omega) + \hat{a}_i^\dagger(\omega) f_i^*(\omega)], \quad (58)$$

where the annihilation and creation operators $\hat{a}_i(\omega)$, $\hat{a}_i^\dagger(\omega)$ satisfy the equal-time commutation relations

$$\begin{aligned} [\hat{a}_i, \hat{a}_{i'}] &= 0 \\ [\hat{a}_i^\dagger, \hat{a}_{i'}^\dagger] &= 0 \\ [\hat{a}_i, \hat{a}_{i'}^\dagger] &= \delta(i - i'), \end{aligned} \quad (59)$$

valid for free scalar fields quantized on equal-time hypersurfaces in curved spacetime.

The Rindler vacuum $|0_{R_i}\rangle$ associated with the mode set i is defined by

$$\hat{a}_i(\omega) |0_{R_i}\rangle = 0, \quad \forall \omega. \quad (60)$$

Similarly, one can expand $\hat{\Phi}$ in the basis $\{f_j(\Omega)\}$,

$$\hat{\Phi} = \int_{-\infty}^{\infty} d\Omega [\hat{a}_j(\Omega) f_j(\Omega) + \hat{a}_j^\dagger(\Omega) f_j^*(\Omega)], \quad (61)$$

with the annihilation and creation operators $\hat{a}_j(\Omega)$, $\hat{a}_j^\dagger(\Omega)$ satisfying the same commutation relations as in Eq. (59), and associated vacuum $|0_{R_j}\rangle$ obeying

$$\hat{a}_j(\Omega) |0_{R_j}\rangle = 0, \quad \forall \Omega. \quad (62)$$

Using the Bogoliubov transformations (56) and (57), the annihilation and creation operators transform as

$$\hat{a}_j(\Omega) = \int_0^{\infty} d\omega [\alpha_{ji}^*(\Omega, \omega) \hat{a}_i(\omega) - \beta_{ji}^*(\Omega, \omega) \hat{a}_i^\dagger(\omega)], \quad (63)$$

$$\hat{a}_j^\dagger(\Omega) = \int_0^{\infty} d\omega [\alpha_{ji}(\Omega, \omega) \hat{a}_i^\dagger(\omega) - \beta_{ji}(\Omega, \omega) \hat{a}_i(\omega)]. \quad (64)$$

When the β -coefficients are non-zero, the particle number operator expectation value evaluated in the vacuum $|0_{R_i}\rangle$ associated with the i -modes is

$$\langle 0_{R_i} | \hat{N}_{ji}(\Omega) | 0_{R_i} \rangle = \langle 0_{R_i} | \hat{a}_j^\dagger(\Omega) \hat{a}_j(\Omega) | 0_{R_i} \rangle = \int d\omega |\beta_{ji}(\Omega, \omega)|^2, \quad (65)$$

which demonstrates that an observer associated with the j -modes detects particles in the vacuum defined by the i -modes whenever $\beta_{ji} \neq 0$.

In this section, we derive the Bogoliubov transformation between two complete sets of mode functions and use it to evaluate the expectation value of the number operator in different Rindler frames.

C. Virasoro anamoly method

In two dimensions, all components of $\langle T_{\mu\nu} \rangle$ can be determined using the Virasoro anomaly of the normal-ordered stress tensor. While normal ordering is well defined in Minkowski spacetime, its extension to curved spacetime can be motivated by applying it in locally inertial frames, which exist at each spacetime point. This prescription is consistent with general covariance and enables the determination of all components of the covariant quantum stress tensor.

A potential subtlety arises from the use of local coordinates, since the definition of a quantum state is intrinsically global. In particular, normal ordering with respect to positive-frequency modes $\frac{1}{\sqrt{4\pi\omega}} e^{-i\omega u}$ and $\frac{1}{\sqrt{4\pi\omega}} e^{-i\omega v}$ defined in local coordinates may appear ambiguous from a global standpoint. In semiclassical gravity, this issue is addressed by restricting to Hadamard states, for which the short-distance singularity structure of the two-point function is locally Minkowskian and admits a consistent renormalisation prescription [11–13].

In this work, we employ Rindler coordinates, which cover only a portion of Minkowski spacetime. Nonetheless, the normal-ordered stress tensor is well defined within the Rindler wedge and corresponds to renormalisation with respect to the Rindler vacuum [10]. The resulting expectation values have a clear operational interpretation in terms of observables accessible to uniformly accelerated observers and are directly related to the Unruh effect [1, 14, 15]. This restriction to the Rindler wedge does not compromise the consistency of the semi-classical description.

Under conformal transformation $f(u)$, the energy-momentum tensor behaves as

$$T'(u) = \left(\frac{\partial f}{\partial u} \right)^2 T(f(u)) + \frac{c}{12} S(U, u)$$

Where $S(U, u)$ denotes the Schwarzian derivative and is defined as [16]:

$$S(U, u) = (1/\partial_u U)^2 [(\partial_u U)(\partial_u^3 U) - \frac{3}{2}(\partial_u^2 U)^2], \quad (66)$$

And, c denotes the central charge.

IV. PARTICLE CONTENT IN R_3 ALONG VARIOUS PATHS

In this section, we analyse, in a unified and comparative manner, the particle content detected by an accelerated observer confined to the fixed Rindler wedge R_3 along four inequivalent construction paths. In each case, the notion of particles is defined with respect to the positive-frequency Rindler modes adapted to R_3 , and thermality is diagnosed operationally through the expectation values of the corresponding number operators. While all four paths can give rise to thermal particle spectra in R_3 , the physical origin of this thermality differs markedly among them. In particular, we distinguish between thermality arising from horizon-induced entanglement, which leads to a mixed Gibbs state and thermalisation of both chiral sectors, and thermality generated purely by Bogoliubov mixing under null-shift transformations, which produces a thermal spectrum in only one chiral sector while the global and local quantum states remain pure. By keeping the final wedge R_3 fixed and varying only the global state and the sequence of coordinate transformations, we isolate the mechanisms responsible for full versus selective thermalisation in Rindler spacetime.

A. Particle content along path 1

In this section, we evaluate the particle content along Path 1, focusing on the particle content in R_3 when the field is in the Minkowski vacuum. The wedge R_3 is spatially shifted from the origin by a parameter Δ_1 , as illustrated in Figs. 1 and 2. Since the Unruh effect is invariant under such spatial translations, we expect the particle content in R_3 to be thermal. We demonstrate this explicitly below.

The light-cone coordinates are related as in Eqs. (7) and (8). The right-moving and left-moving components of the Minkowski field operator $\hat{\phi}_0$ can be expanded as:

$$\hat{\phi}_0(U_M) = \int_0^\infty \frac{d\omega_0}{\sqrt{4\pi\omega_0}} \left[\vec{a}_0(\omega_0) e^{-i\omega_0 U_M} + \vec{a}_0^\dagger(\omega_0) e^{i\omega_0 U_M} \right], \quad (67)$$

$$\hat{\phi}_0(V_M) = \int_0^\infty \frac{d\omega_0}{\sqrt{4\pi\omega_0}} \left[\vec{b}_0(\omega_0) e^{-i\omega_0 V_M} + \vec{b}_0^\dagger(\omega_0) e^{i\omega_0 V_M} \right]. \quad (68)$$

Starting from Eq. (50), we multiply both sides by $\int_{-\infty}^\infty \frac{du_3}{\sqrt{2\pi}} e^{i\nu' u_3}$, resulting in

$$\int_{-\infty}^\infty \frac{du_3}{\sqrt{2\pi}} e^{i\nu' u_3} \hat{\phi}_3 = \int_0^\infty \frac{d\nu}{\sqrt{2\pi}} \frac{1}{\sqrt{2\nu}} \int_{-\infty}^\infty \frac{du_3}{\sqrt{2\pi}} \left(\vec{a}_3(\nu) e^{i(\nu' - \nu) u_3} + \vec{a}_3^\dagger(\nu) e^{i(\nu + \nu') u_3} \right), \quad (69)$$

For $\nu' > 0$, only the first term contributes due to orthogonality, yielding:

$$\int_{-\infty}^\infty \frac{du_3}{\sqrt{2\pi}} e^{i\nu' u_3} \hat{\phi}_3 = \frac{\vec{a}_3(\nu')}{\sqrt{2\nu'}}. \quad (70)$$

We now compute the same integral using the Minkowski field operator $\hat{\phi}_0$ from Eq. (67),

$$\int_{-\infty}^\infty \frac{du_3}{\sqrt{2\pi}} e^{i\nu' u_3} \hat{\phi}_0 = \frac{1}{2\pi} \int_0^\infty \frac{d\omega_0}{\sqrt{2\omega_0}} \int_{-\infty}^\infty du_3 \left(\vec{a}_0(\omega_0) e^{-i\omega_0 U_M} e^{i\nu' u_3} + \vec{a}_0^\dagger(\omega_0) e^{i\omega_0 U_M} e^{i\nu' u_3} \right), \quad (71)$$

Setting $\nu' = \nu > 0$, and substituting U_M from Eq. (7) at $a_3 = a$ and $\Delta_1 = \frac{1}{a}$, we identify the Bogoliubov coefficients by matching Eq. (63),

$$\vec{\alpha}_{30}^*(\nu, \omega_0) = \sqrt{\frac{\nu}{\omega_0}} \int_{-\infty}^\infty \frac{du_3}{2\pi} e^{i\omega_0 u_3} (e^{-au_3} + 1)^{i\nu/a} e^{i\nu u_3}, \quad (72)$$

$$\vec{\beta}_{30}^*(\nu, \omega_0) = -\sqrt{\frac{\nu}{\omega_0}} \int_{-\infty}^\infty \frac{du_3}{2\pi} e^{-i\omega_0 u_3} (e^{-au_3} + 1)^{i\nu/a} e^{i\nu u_3}. \quad (73)$$

After evaluation, these integrals yield expressions involving Gamma functions:

$$\vec{\alpha}_{30}^*(\nu, \omega_0) = \frac{1}{2\pi a} \sqrt{\frac{\nu}{\omega_0}} e^{i\omega_0 \frac{\nu}{a}} \Gamma\left(-\frac{i\nu}{a}\right) \left(\frac{-i\omega_0}{a}\right)^{\frac{i\nu}{a}}, \quad (74)$$

$$\vec{\beta}_{30}^*(\nu, \omega_0) = -\frac{1}{2\pi a} \sqrt{\frac{\nu}{\omega_0}} e^{-i\omega_0 \frac{\nu}{a}} \Gamma\left(-\frac{i\nu}{a}\right) \left(\frac{i\omega_0}{a}\right)^{\frac{i\nu}{a}}. \quad (75)$$

The Minkowski vacuum $|0_M\rangle$ is defined by

$$\vec{a}_0(\omega_0)|0_M\rangle = 0, \quad \vec{b}_0(\omega_0)|0_M\rangle = 0, \quad (76)$$

where the annihilation operators satisfy the commutation relations as per Eq. (59).

The expectation value of the right-moving particle number operator $\vec{N}_{30}(\nu) = \vec{a}_3^\dagger(\nu) \vec{a}_3(\nu)$ in the Minkowski vacuum is given by

$$\langle 0_M | \vec{N}_{30}(\nu) | 0_M \rangle = \int_0^\infty d\omega_0 \left| \vec{\beta}_{30}(\nu, \omega_0) \right|^2, \quad (77)$$

which simplifies to the Planckian distribution

$$\langle \vec{N}_{30}(\nu) \rangle = \frac{\delta(0)}{e^{\frac{2\pi\nu}{a}} - 1}, \quad (78)$$

where the formal divergence $\delta(0)$ arises from the infinite volume and is treated as a constant in a finite volume

(see Appendix B). The corresponding particle number density reads [17]

$$\vec{n}_{30}(\nu) = \frac{1}{e^{\frac{2\pi\nu}{a}} - 1}. \quad (79)$$

Thus, the right-moving modes in wedge R_3 , when evaluated in the Minkowski vacuum, are thermally excited and exhibit a Planck distribution. A similar calculation shows that the left-moving modes also thermalize, confirming full thermality along Path 1.

This thermal mixed state arises because the Minkowski vacuum is entangled between modes inside R_3 and those in its complement; tracing over inaccessible modes yields a thermal reduced state.

For subsequent sections, we take the initial state to be the vacuum $|0_{R_1}\rangle$ defined with respect to positive frequency Rindler modes localized entirely in the right wedge R_1 :

$$\vec{a}_1(\omega)|0_{R_1}\rangle = 0, \quad \overleftarrow{b}_1(\omega)|0_{R_1}\rangle = 0. \quad (80)$$

Here, $\vec{a}_1(\omega)$ and $\overleftarrow{b}_1(\omega)$ annihilate right- and left-moving modes in R_1 , respectively.

For an R_1 observer, the expectation values of particle number operators vanish:

$$\langle 0_{R_1} | \vec{N}_{R_1}(\omega) | 0_{R_1} \rangle = 0, \quad \langle 0_{R_1} | \overleftarrow{N}_{R_1}(\omega) | 0_{R_1} \rangle = 0.$$

Since the left wedge degrees of freedom are excluded in our construction, the $|0_{R_1}\rangle$ state remains pure and unentangled, with no partial trace performed. Hence, the standard Unruh mechanism involving tracing over inaccessible modes does not operate here [18]. We adopt this scenario as a baseline: in the R_1 vacuum, an observer detects no particles, and thermality observed later is defined relative to this baseline.

B. Particle content along path 2

In this section, we evaluate the particle content along Path 2, which connects the Rindler wedges R_1 and R_3 through a spatial shift parametrized by Δ_1 , as illustrated in Figs. 1 and 2. To compute the Bogoliubov coefficients relating the mode functions in these two wedges, we proceed as follows.

Starting from Eq. (50), we multiply both sides by $\int_{-\infty}^{\infty} \frac{du_3}{\sqrt{2\pi}} e^{i\nu' u_3}$, yielding

$$\begin{aligned} \int_{-\infty}^{\infty} \frac{du_3}{\sqrt{2\pi}} e^{i\nu' u_3} \hat{\phi}_3 &= \int_0^{\infty} \frac{d\nu}{\sqrt{2\pi}} \frac{1}{\sqrt{2\nu}} \\ \int_{-\infty}^{\infty} \frac{du_3}{\sqrt{2\pi}} \left(\vec{a}_3(\nu) e^{i(\nu' - \nu) u_3} + \vec{a}_3^\dagger(\nu) e^{i(\nu + \nu') u_3} \right), \end{aligned} \quad (81)$$

where, for $\nu' > 0$, only the first term contributes due to orthogonality, giving

$$\int_{-\infty}^{\infty} \frac{du_3}{\sqrt{2\pi}} e^{i\nu' u_3} \hat{\phi}_3 = \frac{\vec{a}_3(\nu')}{\sqrt{2\nu'}}. \quad (82)$$

Computing the same quantity using the field operator in wedge R_1 , Eq. (48), and multiplying by the same factor,

$$\begin{aligned} \int_{-\infty}^{\infty} \frac{du_3}{\sqrt{2\pi}} e^{i\nu' u_3} \hat{\phi}_1 &= \frac{1}{2\pi} \int_0^{\infty} \frac{d\omega}{\sqrt{2\omega}} \int_{-\infty}^{\infty} du_3 \\ \left(\vec{a}_1(\omega) e^{-i\omega u_1} e^{i\nu' u_3} + \vec{a}_1^\dagger(\omega) e^{i\omega u_1} e^{i\nu' u_3} \right), \end{aligned} \quad (83)$$

Setting $\nu' = \nu > 0$ and comparing with Eq. (82), we obtain:

$$\begin{aligned} \vec{a}_3(\nu) &= \int_0^{\infty} d\omega \left[\vec{a}_1(\omega) \sqrt{\frac{\nu}{\omega}} \int_{-\infty}^{\infty} \frac{du_3}{2\pi} e^{-i\omega u_1} e^{i\nu u_3} \right. \\ &\quad \left. + \vec{a}_1^\dagger(\omega) \sqrt{\frac{\nu}{\omega}} \int_{-\infty}^{\infty} \frac{du_3}{2\pi} e^{i\omega u_1} e^{i\nu u_3} \right]. \end{aligned} \quad (84)$$

By matching with Eq. (63), the Bogoliubov coefficients follow as:

$$\vec{\alpha}_{31}^*(\nu, \omega) = \sqrt{\frac{\nu}{\omega}} \int_{-\infty}^{\infty} \frac{du_3}{2\pi} e^{-i\omega u_1} e^{i\nu u_3}, \quad (85)$$

$$\vec{\beta}_{31}^*(\nu, \omega) = -\sqrt{\frac{\nu}{\omega}} \int_{-\infty}^{\infty} \frac{du_3}{2\pi} e^{i\omega u_1} e^{i\nu u_3}. \quad (86)$$

Using the relation between coordinates u_1 and u_3 from Eq. (11) and simplifying, we obtain:

$$\vec{\alpha}_{31}^*(\nu, \omega) = \frac{1}{2\pi a} \sqrt{\frac{\nu}{\omega}} \frac{\Gamma\left(\frac{i\nu}{a}\right) \Gamma\left(-\frac{i(\nu+\omega)}{a}\right)}{\Gamma\left(-\frac{i\omega}{a}\right)}, \quad (87)$$

$$\vec{\beta}_{31}^*(\nu, \omega) = -\frac{1}{2\pi a} \sqrt{\frac{\nu}{\omega}} \frac{\Gamma\left(-\frac{i\nu}{a}\right) \Gamma\left(\frac{i(\nu+\omega)}{a}\right)}{\Gamma\left(\frac{i\omega}{a}\right)}. \quad (88)$$

Squaring the modulus of $\vec{\beta}_{31}$, we have

$$|\vec{\beta}_{31}(\nu, \omega)|^2 = \vec{\beta}_{31}^*(\nu, \omega) \vec{\beta}_{31}(\nu, \omega), \quad (89)$$

which simplifies to

$$|\vec{\beta}_{31}(\nu, \omega)|^2 = \frac{1}{4\pi a} \frac{\sinh\left(\frac{\pi\omega}{a}\right)}{(\omega + \nu) \sinh\left(\frac{\pi\nu}{a}\right) \sinh\left(\frac{\pi(\omega+\nu)}{a}\right)}. \quad (90)$$

Defining the vacuum state from Eqs. (60) and (62),

$$\vec{a}_1(\omega)|0_{R_1}\rangle = 0,$$

where the operators satisfy commutation relations as in Eq. (59).

The expectation value of the number operator in the vacuum $|0_{R_1}\rangle$ is [19, 20]

$$\langle 0_{R_1} | \vec{a}_3^\dagger(\nu) \vec{a}_3(\nu) | 0_{R_1} \rangle = \int_0^\infty d\omega |\vec{\beta}_{31}(\nu, \omega)|^2. \quad (91)$$

Substituting Eq. (90) into the above integral yields

$$\langle \vec{N}_{31}(\nu) \rangle = \frac{1}{4\pi a \sinh(\frac{\pi\nu}{a})} \int_0^\infty d\omega \frac{\sinh(\frac{\pi\omega}{a})}{(\omega + \nu) \sinh(\frac{\pi(\omega+\nu)}{a})}, \quad (92)$$

which, using the integral result from Appendix B, evaluates to

$$\langle \vec{N}_{31}(\nu) \rangle = \frac{\delta(0)}{e^{\frac{2\pi\nu}{a}} - 1}, \quad (93)$$

with $\delta(0)$ representing the infinite mode density in the unbounded spatial volume [9]. The corresponding mean particle number density is [17]

$$\vec{n}_{31}(\nu) = \frac{1}{e^{\frac{2\pi\nu}{a}} - 1}. \quad (94)$$

Hence, the right-moving modes in wedge R_3 , evaluated from the vacuum of R_1 , are thermally excited and exhibit a Planckian distribution. A similar calculation for the left-moving modes confirms their thermal excitation, establishing full thermalisation of both modes along Path 2.

The resulting mixed state arises because the vacuum $|0_{R_1}\rangle$ is entangled between modes inside the wedge and their complementary modes, with tracing over inaccessible regions yielding a thermal reduced state in R_3 .

C. Path 3. Particle content along shifts along V_1 and U_2 axes respectively

In this section, we evaluate the Bogoliubov transformations and the resulting particle content along Path 3, where the Rindler wedge R_2 is obtained from R_1 by a null shift along the V_1 -axis, and R_3 is subsequently obtained from R_2 along the U_2 -axis, as illustrated in Fig. 1. Thus, the evaluation of particle content in R_3 from the vacuum in R_1 proceeds in two stages, with the intermediate wedge R_2 serving as a pitstop.

To calculate the required Bogoliubov coefficients, we begin by multiplying both sides of Eq. (47) by the Fourier kernel $\int_{-\infty}^\infty \frac{du_2}{\sqrt{2\pi}} e^{i\Omega' u_2}$. After simplifications and using the orthogonality of exponentials, we obtain [21]

$$\begin{aligned} \int_{-\infty}^\infty \frac{du_2}{\sqrt{2\pi}} e^{i\Omega' u_2} \hat{\phi}_2 &= \int_0^\infty \frac{d\Omega}{\sqrt{2\pi}} \frac{1}{\sqrt{2\Omega}} \\ \int_{-\infty}^\infty \frac{du_2}{\sqrt{2\pi}} \left(\vec{a}_2(\Omega) e^{i(\Omega' - \Omega) u_2} + \vec{a}_2^\dagger(\Omega) e^{i(\Omega + \Omega') u_2} \right), \end{aligned} \quad (95)$$

Which reduces to

$$\int_{-\infty}^\infty \frac{du_2}{\sqrt{2\pi}} e^{i\Omega' u_2} \hat{\phi}_2 = \frac{\vec{a}_2(\Omega')}{\sqrt{2\Omega'}}, \quad (96)$$

Due to orthogonality, valid for $\Omega' > 0$.

Next, we compute the same integral using the field operator $\hat{\phi}_1(u_1)$, expressed in terms of u_2 via the null-shift relation connecting wedges R_1 and R_2 . Multiplying both sides of Eq. (46) by the same Fourier kernel gives

$$\begin{aligned} \int_{-\infty}^\infty \frac{du_2}{\sqrt{2\pi}} e^{i\Omega' u_2} \hat{\phi}_1 &= \frac{1}{2\pi} \int_0^\infty \frac{d\omega}{\sqrt{2\omega}} \left(\vec{a}_1(\omega) \int_{-\infty}^\infty du_2 \right. \\ &\quad \left. e^{i\Omega' u_2 - i\omega u_1} + \vec{a}_1^\dagger(\omega) \int_{-\infty}^\infty du_2 e^{i\Omega' u_2 + i\omega u_1} \right), \end{aligned} \quad (97)$$

Matching Eqs. (96) and (97), and evaluating at $\Omega' = \Omega$, allows us to identify the Bogoliubov coefficients between wedges R_1 and R_2 :

$$\vec{\alpha}_{21}^*(\Omega, \omega) = \sqrt{\frac{\Omega}{\omega}} \int_{-\infty}^\infty \frac{du_2}{2\pi} e^{i\Omega u_2 - i\omega u_1}, \quad (98)$$

$$\vec{\beta}_{21}^*(\Omega, \omega) = -\sqrt{\frac{\Omega}{\omega}} \int_{-\infty}^\infty \frac{du_2}{2\pi} e^{i\Omega u_2 + i\omega u_1}. \quad (99)$$

Utilizing the explicit coordinate transformation between u_1 and u_2 from Eq. (21), one finds that

$$\vec{\alpha}_{21}^*(\Omega, \omega) = \delta(\Omega - \omega) \sqrt{\frac{\Omega}{\omega}}, \quad (100)$$

and

$$\vec{\beta}_{21}^*(\Omega, \omega) = 0. \quad (101)$$

This confirms that, for the right-moving modes, the null shift from R_1 to R_2 does not excite particles; the vacuum structure remains preserved.

We now compute the Bogoliubov coefficients for the left-moving modes relating the Rindler wedges R_1 and R_2 . Starting from the transformation relations and Eq. (63), the coefficient $\overleftarrow{\alpha}_{21}^*(\Omega, \omega)$ is expressed as

$$\overleftarrow{\alpha}_{21}^*(\Omega, \omega) = \frac{1}{2\pi} \sqrt{\frac{\Omega}{\omega}} \int_{-\infty}^\infty dv_2 e^{i\Omega v_2} e^{-\frac{i\omega}{a} \ln[e^{\alpha v_2} + 1]}, \quad (102)$$

which simplifies through standard integration techniques (see Appendix A) to

$$\overleftarrow{\alpha}_{21}^*(\Omega, \omega) = \frac{1}{2\pi a} \sqrt{\frac{\Omega}{\omega}} \frac{2^{-\frac{i\omega+i\Omega}{a}} \Gamma\left(\frac{i\Omega}{a}\right) \Gamma\left(\frac{i\omega-i\Omega}{a}\right)}{\Gamma\left(\frac{i\omega}{a}\right)}. \quad (103)$$

Similarly, the Bogoliubov coefficient $\overleftarrow{\beta}_{21}^*(\Omega, \omega)$ is given by

$$\overleftarrow{\beta}_{21}^*(\Omega, \omega) = -\frac{1}{2\pi} \sqrt{\frac{\Omega}{\omega}} \int_{-\infty}^\infty dv_2 e^{i\Omega v_2} e^{i\omega v_1}, \quad (104)$$

and evaluates to

$$\overleftarrow{\beta}_{21}^*(\Omega, \omega) = -\frac{1}{2\pi a} \sqrt{\frac{\Omega}{\omega}} \frac{2^{\frac{i(\omega+\Omega)}{a}} \Gamma\left(\frac{i\Omega}{a}\right) \Gamma\left(-\frac{i(\omega+\Omega)}{a}\right)}{\Gamma\left(-\frac{i\omega}{a}\right)}. \quad (105)$$

The squared modulus of the Bogoliubov coefficient is

$$\left| \overleftarrow{\beta}_{21}(\Omega, \omega) \right|^2 = \overleftarrow{\beta}_{21}^*(\Omega, \omega) \overleftarrow{\beta}_{21}(\Omega, \omega), \quad (106)$$

Which simplifies to

$$\left| \overleftarrow{\beta}_{21}(\Omega, \omega) \right|^2 = \frac{1}{4\pi^2 a^2} \frac{\Omega}{\omega} \frac{\left| \Gamma\left(\frac{i\Omega}{a}\right) \right|^2 \left| \Gamma\left(\frac{i(\Omega+\omega)}{a}\right) \right|^2}{\left| \Gamma\left(\frac{i\omega}{a}\right) \right|^2}. \quad (107)$$

Applying standard identities for Gamma functions, the above expression reduces to

$$\left| \overleftarrow{\beta}_{21}(\Omega, \omega) \right|^2 = \frac{1}{4\pi a} \frac{\sinh\left(\frac{\pi\omega}{a}\right)}{(\omega + \Omega) \sinh\left(\frac{\pi\Omega}{a}\right) \sinh\left[\frac{\pi(\omega+\Omega)}{a}\right]}. \quad (108)$$

The Rindler vacuum in wedge R_1 is defined by the annihilation condition

$\overleftarrow{\hat{b}}_1 |0_{R_1}\rangle = 0$, and factorises as $|0_{R_1}\rangle = |\overleftarrow{0}_{R_1}\rangle \otimes |\overrightarrow{0}_{R_1}\rangle$, where $|\overleftarrow{0}_{R_1}\rangle$ and $|\overrightarrow{0}_{R_1}\rangle$ denote the left- and right-moving vacuum states, respectively. The operators $\overleftarrow{\hat{b}}_1$ and $\overleftarrow{\hat{b}}_1^\dagger$ satisfy canonical commutation relations analogous to those in Eq. (59).

We then compute the particle content in the left-moving modes of R_2 when the field is in the R_1 vacuum. The expectation value of the number operator is

$$\langle 0_{R_1} | \overleftarrow{\hat{b}}_2^\dagger(\Omega) \overleftarrow{\hat{b}}_2(\Omega) | 0_{R_1} \rangle = \int_0^\infty d\omega \left| \overleftarrow{\beta}_{21}(\Omega, \omega) \right|^2, \quad (109)$$

Which, upon substituting Eq. (108), becomes

$$\langle \overleftarrow{N}_{21}(\Omega) \rangle = \frac{1}{4\pi a \sinh\left(\frac{\pi\Omega}{a}\right)} \int_0^\infty d\omega \frac{\sinh\left(\frac{\pi\omega}{a}\right)}{(\omega + \Omega) \sinh\left[\frac{\pi(\omega+\Omega)}{a}\right]}. \quad (110)$$

This integral is analytically tractable (see Appendix B) and evaluates to

$$\langle \overleftarrow{N}_{21}(\Omega) \rangle = \frac{\delta(0)}{e^{\frac{2\pi\Omega}{a}} - 1}. \quad (111)$$

Here, $\delta(0)$ formally arises from the infinite volume limit and can be interpreted as a constant density over a finite spacetime volume [9]. Accordingly, the mean particle number density for frequency Ω is given by the Planckian distribution [17]:

$$\overleftarrow{n}_{21}(\Omega) = \frac{1}{e^{\frac{2\pi\Omega}{a}} - 1}. \quad (112)$$

This confirms that the left-moving modes are thermally excited during the transition from R_1 to R_2 , at

a characteristic Unruh-like temperature $T = \frac{a}{2\pi}$. In contrast, the right-moving modes remain in the vacuum state.

We now evaluate the particle content of the right-moving modes in the transition from Rindler wedge R_2 to wedge R_3 . The mode functions in R_3 are related to those in R_2 . Setting $j = 3$, $i = 2$, and identifying $\omega = \Omega$, $\nu = \Omega$ in Eqs. (63) and (64), the Bogoliubov coefficients for the right-moving mode are given by:

$$\overrightarrow{\alpha}_{32}^*(\nu, \Omega) = \sqrt{\frac{\nu}{\Omega}} \int_{-\infty}^\infty \frac{du_3}{2\pi} e^{i\nu u_3} e^{-i\Omega u_2}, \quad (113)$$

$$\overrightarrow{\beta}_{32}^*(\nu, \Omega) = -\sqrt{\frac{\nu}{\Omega}} \int_{-\infty}^\infty \frac{du_3}{2\pi} e^{i\nu u_3} e^{i\Omega u_2}. \quad (114)$$

Using the coordinate transformation from Eq. (31), Eq. (113) becomes:

$$\overrightarrow{\alpha}_{32}^*(\nu, \Omega) = \frac{1}{2\pi} \sqrt{\frac{\nu}{\Omega}} \int_{-\infty}^\infty du_3 e^{i\nu u_3} e^{\frac{i\Omega}{a} \ln(e^{-a u_3} + 1)}, \quad (115)$$

which evaluates, using standard techniques (see Appendix A), to

$$\overrightarrow{\alpha}_{32}^*(\nu, \Omega) = \frac{1}{2\pi a} \sqrt{\frac{\nu}{\Omega}} \frac{2^{\frac{i(\Omega-\nu)}{a}} \Gamma\left(-\frac{i\nu}{a}\right) \Gamma\left(\frac{i(\nu-\Omega)}{a}\right)}{\Gamma\left(-\frac{i\Omega}{a}\right)}. \quad (116)$$

Similarly, using Eq. (34), Eq. (114) becomes:

$$\overrightarrow{\beta}_{32}^*(\nu, \Omega) = -\frac{1}{2\pi} \sqrt{\frac{\nu}{\Omega}} \int_{-\infty}^\infty du_3 e^{i\nu u_3} e^{-\frac{i\Omega}{a} \ln(e^{-a u_3} + 1)}, \quad (117)$$

which evaluates to

$$\overrightarrow{\beta}_{32}^*(\nu, \Omega) = -\frac{1}{2\pi a} \sqrt{\frac{\nu}{\Omega}} \frac{2^{-\frac{i(\Omega-\nu)}{a}} \Gamma\left(-\frac{i\nu}{a}\right) \Gamma\left(\frac{i(\nu+\Omega)}{a}\right)}{\Gamma\left(\frac{i\Omega}{a}\right)}. \quad (118)$$

The squared modulus of the Bogoliubov coefficient is

$$\left| \overrightarrow{\beta}_{32}(\nu, \Omega) \right|^2 = \overrightarrow{\beta}_{32}^*(\nu, \Omega) \overrightarrow{\beta}_{32}(\nu, \Omega), \quad (119)$$

which simplifies to

$$\left| \overrightarrow{\beta}_{32}(\nu, \Omega) \right|^2 = \frac{1}{4\pi a} \frac{\sinh\left(\frac{\pi\Omega}{a}\right)}{(\nu + \Omega) \sinh\left(\frac{\pi\nu}{a}\right) \sinh\left[\frac{\pi(\nu+\Omega)}{a}\right]}. \quad (120)$$

Since R_2 is obtained from R_1 through a null shift, the resulting quantum field configuration exhibits selective thermalisation, the left-moving modes become thermally populated, while the right-moving modes remain in vacuum, as previously established. The corresponding quantum state in R_2 factorizes as a tensor product in the Hilbert space \mathcal{H}_{R_2} and is expressed as [10]

$$| \psi_{R_2} \rangle = \left(\sum_{n=0}^\infty \sqrt{p_n} | \overleftarrow{n} \rangle \right) \otimes | \overrightarrow{0} \rangle, \quad (121)$$

where $p_n = \frac{e^{-n\beta\Omega}}{Z}$, $Z = \sum_{n=0}^{\infty} e^{-n\beta\Omega}$, denote the thermal weights and partition function, ensuring $|\psi_{R_2}\rangle$ is normalized [22, Ch. I, §1.3-1.4], [23, Ch. 7]. Here, $|\vec{n}\rangle$ is the n -particle Fock basis state of the left-moving mode, and $|\vec{0}\rangle$ is the vacuum state of the right-moving mode in R_2 . A detailed discussion of this state's structure and its relation to thermal density matrices and purification is provided in Appendix C.

We now compute the expectation value of the number operator for right-moving modes in R_3 evaluated in the state $|\psi_{R_2}\rangle$. The number operator

$$\vec{N}_{32}(\nu) = \vec{a}_3^\dagger(\nu) \vec{a}_3(\nu)$$

has expectation value

$$\langle \vec{N}_{32}(\nu) \rangle = \langle \psi_{R_2} | \vec{a}_3^\dagger(\nu) \vec{a}_3(\nu) | \psi_{R_2} \rangle. \quad (122)$$

Expressed in terms of Bogoliubov coefficients, this is

$$\begin{aligned} \langle \vec{N}_{32}(\nu) \rangle &= \int_0^\infty d\Omega \int_0^\infty d\Omega' \vec{\beta}_{32}^*(\nu, \Omega) \vec{\beta}_{32}(\nu, \Omega') \\ &\quad \times \langle \psi_{R_2} | \vec{a}_2(\Omega') \vec{a}_2^\dagger(\Omega) | \psi_{R_2} \rangle. \end{aligned} \quad (123)$$

Since $|\psi_{R_2}\rangle$ is a tensor product with the right-moving mode in vacuum, the two-point function reduces to

$$\begin{aligned} \langle \psi_{R_2} | \vec{a}_2(\Omega') \vec{a}_2^\dagger(\Omega) | \psi_{R_2} \rangle &= \langle \vec{0} | \vec{a}_2(\Omega') \vec{a}_2^\dagger(\Omega) | \vec{0} \rangle \\ &= \delta(\Omega - \Omega'). \end{aligned} \quad (124)$$

Therefore, the expectation value reduces to

$$\langle \vec{N}_{32}(\nu) \rangle = \int_0^\infty d\Omega \left| \vec{\beta}_{32}(\nu, \Omega) \right|^2, \quad (125)$$

which, by substitution of Eq. (120), is an integral of the same form as in Eq. (110). Evaluating this integral (see Appendix B) gives

$$\langle \vec{N}_{32}(\nu) \rangle = \frac{\delta(0)}{e^{\frac{2\pi\nu}{a}} - 1}. \quad (126)$$

The factor $\delta(0)$ arises from the mode normalization in the continuum and represents an infinite constant related to the volume. Hence, the mean particle number density per unit frequency ν in R_3 , as measured in R_2 , is

$$\vec{n}_{32}(\nu) = \frac{1}{e^{\frac{2\pi\nu}{a}} - 1}, \quad (127)$$

expressing the familiar Planckian distribution at the Unruh-like temperature $T = \frac{a}{2\pi}$.

We conclude that the right-moving modes mediating between R_2 and R_3 exhibit a thermal population characterized by this Planckian spectrum when the field in R_2 is selectively excited state $|\psi_{R_2}\rangle$.

We now evaluate the particle content of the left-moving modes in the transition from Rindler wedge R_2 to wedge

R_3 . The Bogoliubov coefficients relating the mode functions across these regions are given by:

$$\vec{\alpha}_{32}^*(\nu, \Omega) = \sqrt{\frac{\nu}{\Omega}} \int_{-\infty}^{\infty} \frac{dv_3}{2\pi} e^{i\nu v_3} e^{-i\Omega v_2}, \quad (128)$$

$$\vec{\beta}_{32}^*(\nu, \Omega) = -\sqrt{\frac{\nu}{\Omega}} \int_{-\infty}^{\infty} \frac{dv_3}{2\pi} e^{i\nu v_3} e^{i\Omega v_2}, \quad (129)$$

The coordinate relation between the wedges, as given by Eq. (32), implies $v_2 = v_3$. Substituting this into the expressions above and evaluating the integrals, we find:

$$\vec{\alpha}_{32}^*(\nu, \Omega) = \sqrt{\frac{\nu}{\Omega}} \delta(\nu - \Omega), \quad (130)$$

And;

$$\vec{\beta}_{32}^*(\nu, \Omega) = 0, \quad (131)$$

Hence, the left-moving modes in wedge R_2 remain in vacuum when mapped to a wedge R_3 ; no particle creation occurs in this region. This is consistent with the preservation of the positive-frequency structure of the modes under the coordinate transformation.

We now examine the particle content in region R_3 as seen from the vacuum defined in region R_1 , by following the composite path $R_1 \rightarrow R_2 \rightarrow R_3$ (Path 3). The state in R_1 is taken to be the Rindler vacuum, satisfying

$$\vec{a}_1 |0_{R_1}\rangle = 0 \quad \text{and} \quad \vec{b}_1 |0_{R_1}\rangle = 0, \quad (132)$$

Along this path, the left-moving modes experience Bogoliubov mixing from R_1 to R_2 , while the right-moving modes undergo mixing from R_2 to R_3 .

a. Composing Bogoliubov Coefficients: To analyze the full transition from R_1 to R_3 , we compose the Bogoliubov coefficients using the substitution of Eq. (57) into Eq. (56), yielding:

$$f_j(\Omega) = \int d\omega \int d\Omega \left[\alpha_{ji}(\Omega, \omega) (\alpha_{ji}^*(\Omega, \omega) f_j(\Omega) - \beta_{ji}(\Omega, \omega) f_j^*(\Omega)) + \beta_{ji}(\Omega, \omega) (\alpha_{ji}(\Omega, \omega) f_j^*(\Omega) - \beta_{ji}^*(\Omega, \omega) f_j(\Omega)) \right],$$

Rearranging terms and comparing with the standard expansion of modes in terms of annihilation and creation operators, we identify the composed Bogoliubov coefficient:

$$\beta_{31}(\nu, \omega) = \int d\Omega [\beta_{32}(\nu, \Omega) \alpha_{21}(\Omega, \omega) - \alpha_{32}(\nu, \Omega) \beta_{21}(\Omega, \omega)]. \quad (133)$$

b. Right-Moving mode: We now examine the right-moving sector. In the second leg of the path, $R_2 \rightarrow R_3$, the Bogoliubov transformation for right-moving modes is nontrivial, while the transformation from $R_1 \rightarrow R_2$ contributes no additional right-moving excitations. Therefore, using Eqs. (100), (101), and (133) for $\Omega, \omega > 0$, the integration simplifies, and we obtain:

$$\vec{\beta}_{31}(\nu, \omega) = \vec{\beta}_{32}(\nu, \omega), \quad (134)$$

Since $\overrightarrow{\beta}_{32}$ corresponds to thermal particle production (as shown previously), it follows that $\overleftarrow{\beta}_{31}$ also exhibits thermal behavior.

c. *Left-Moving mode:* Conversely, for left-moving modes, the thermal contribution arises during the transition from R_1 to R_2 , while the transformation from R_2 to R_3 preserves left-moving vacuum structure. As a result, from Eq. (133) in the left-moving case, we find:

$$\overleftarrow{\beta}_{31}(\nu, \omega) = -\overleftarrow{\beta}_{21}(\nu, \omega), \quad (135)$$

Again, since $\overleftarrow{\beta}_{21}$ is thermal, this confirms that the left-moving modes in region R_3 also appear excited with thermal weight when viewed from the vacuum in R_1 .

We therefore conclude that, along path 3 from region R_1 to R_3 , both the left- and right-moving modes undergo Bogoliubov transformations that excite particles relative to the initial vacuum $|0_{R_1}\rangle$. The left-moving mode acquires thermal excitation through the transition $R_1 \rightarrow R_2$, while the right-moving sector becomes thermal due to the transformation $R_2 \rightarrow R_3$, as demonstrated by Eqs. (134) and (135).

The resulting state in wedge R_3 , as expressed in the number basis of left- and right-moving modes, thus takes the form:

$$|\psi_{R_3}\rangle = \left(\sum_n^{\infty} \sqrt{p_n} |\overleftarrow{n}\rangle \right) \otimes \left(\sum_m^{\infty} \sqrt{q_m} |\overrightarrow{m}\rangle \right), \quad (136)$$

Equation (136) represents a product of two pure states in the Fock space of region R_3 , each expressed as a thermal-like superposition of number eigenstates in the left- and right-moving modes. Although the coefficients p_n and q_m follow thermal occupation distributions, the resulting state is a pure vector in the single-wedge Hilbert space and does not correspond to a mixed Gibbs thermal density matrix. In the present construction, both left- and right-moving modes are supported entirely within a single Rindler wedge and generate the same local field algebra. Since no causally complementary region is traced over, there is no bipartite decomposition of the Hilbert space and hence no entanglement between Rindler wedges along the null shift. Consequently, the selectively excited state remains pure, despite exhibiting a thermal particle spectrum (Bogoliubov-induced superposition of number eigenstates) in one chiral sector.

Importantly, this state is not a purification of a thermal density matrix, nor is it structurally equivalent to a thermofield double, which involves entanglement between left and right modes. Instead, the structure of Eq. (136) arises from independent Bogoliubov excitations in the left- and right-moving modes along the composite path $R_1 \rightarrow R_3$. As a result, the state is a pure [24] and direct tensor product, on the single-wedge Fock space of R_3 . A detailed discussion of the structure and interpretation of this state—including its relation to thermal density matrices and purification—is provided in Appendix D.

D. Particle content along the horizon U_1 and V_2 axes

In this section, we analyze the Bogoliubov transformations and particle content along Path 4, wherein the Rindler wedge R_4 is obtained from R_1 via a null shift along the U_1 -axis, followed by the transition $R_4 \rightarrow R_3$ through a null shift along the V_2 -axis, as depicted in Fig. 2.

Since the method for computing Bogoliubov coefficients has already been established in the previous section, we directly write down the expressions for the transition $R_1 \rightarrow R_4$, which follows the same computational steps. The Bogoliubov coefficients for the right-moving modes are given by:

$$\overrightarrow{\alpha}_{41}^*(\rho, \omega) = \sqrt{\frac{\rho}{\omega}} \int_{-\infty}^{\infty} \frac{du_4}{2\pi} e^{i\rho u_4} e^{-i\omega u_1}, \quad (137)$$

$$\overrightarrow{\beta}_{41}^*(\rho, \omega) = -\sqrt{\frac{\rho}{\omega}} \int_{-\infty}^{\infty} \frac{du_4}{2\pi} e^{i\rho u_4} e^{i\omega u_1}, \quad (138)$$

Where the coordinates u_1 and u_4 are related via Eq. (34).

As these integrals follow the same structure as in the previous section, we state the result directly. The mean number of particles in the right-moving mode of R_4 , when the field is in the vacuum associated with R_1 , is given by:

$$\overrightarrow{n}_{41}(\rho) = \frac{1}{e^{\frac{2\pi\rho}{a}} - 1}, \quad (139)$$

Which is a Planckian distribution at temperature $T = \frac{a}{2\pi}$ arises due to a horizon effect induced by null shifts. This can be regarded as a certain converse of the Unruh effect.

We now evaluate the Bogoliubov coefficients for the left-moving modes associated with the transition $R_1 \rightarrow R_4$:

$$\overleftarrow{\alpha}_{41}^*(\rho, \omega) = \sqrt{\frac{\rho}{\omega}} \int_{-\infty}^{\infty} \frac{dv_4}{2\pi} e^{i\Omega v_4} e^{-i\omega v_1}, \quad (140)$$

$$\overleftarrow{\beta}_{41}^*(\rho, \omega) = -\sqrt{\frac{\rho}{\omega}} \int_{-\infty}^{\infty} \frac{dv_4}{2\pi} e^{i\Omega v_4} e^{i\omega v_1}, \quad (141)$$

Substituting $v_1 = v_4$ from Eq. (34), the integrals simplify to:

$$\overleftarrow{\alpha}_{41}^*(\rho, \omega) = \delta(\rho - \omega) \sqrt{\frac{\rho}{\omega}}, \quad (142)$$

$$\overleftarrow{\beta}_{41}^*(\rho, \omega) = 0, \quad (143)$$

This confirms that no particle creation occurs in the left-moving sector during the transition from $R_1 \rightarrow R_4$.

We conclude that the null shift along the U_1 -axis selectively excites only the right-moving modes in R_4 , while the left-moving modes remain in the vacuum.

We now evaluate the Bogoliubov transformation from R_4 to R_3 for the right-moving mode between regions. As before, the coefficients take the form:

$$\overrightarrow{\alpha}_{34}^*(\nu, \rho) = \sqrt{\frac{\nu}{\rho}} \int_{-\infty}^{\infty} \frac{du_3}{2\pi} e^{i\nu u_3} e^{-i\rho u_4}, \quad (144)$$

$$\overrightarrow{\beta}_{34}^*(\nu, \rho) = -\sqrt{\frac{\nu}{\rho}} \int_{-\infty}^{\infty} \frac{du_3}{2\pi} e^{i\nu u_3} e^{i\rho u_4}, \quad (145)$$

Using the coordinate transformation from Eq. (39) that relates u_3 and u_4 , we find that:

$$\overrightarrow{\alpha}_{34}^*(\nu, \rho) = \delta(\nu - \rho) \sqrt{\frac{\nu}{\rho}}, \quad (146)$$

$$\overrightarrow{\beta}_{34}^*(\nu, \rho) = 0, \quad (147)$$

Hence, the right-moving modes in wedge R_4 remain in vacuum when mapped to wedge R_3 ; no particle creation occurs in this region.

We now evaluate the Bogoliubov coefficients for the left-moving mode associated with the transition from R_4 to R_3 . The mode functions are related via Eqs. (63) and (64), with $j = 3$, $i = 2$, $\Omega = \nu$, and $\omega = \rho$. The Bogoliubov coefficients take the form:

$$\overleftarrow{\alpha}_{34}^*(\nu, \rho) = \sqrt{\frac{\nu}{\rho}} \int_{-\infty}^{\infty} \frac{dv_3}{2\pi} e^{i\nu v_3} e^{-i\rho v_4}, \quad (148)$$

$$\overleftarrow{\beta}_{34}^*(\nu, \rho) = -\sqrt{\frac{\nu}{\rho}} \int_{-\infty}^{\infty} \frac{dv_3}{2\pi} e^{i\nu v_3} e^{i\rho v_4}, \quad (149)$$

Substituting the coordinate transformation from Eq. (40) into the integrals and performing the simplification, we obtain:

$$\overleftarrow{\alpha}_{34}^*(\nu, \Omega) = \frac{1}{2\pi a} \sqrt{\frac{\nu}{\rho}} \frac{2^{\frac{-i(\rho-\nu)}{a}} \Gamma[\frac{i\nu}{a}] \Gamma[\frac{i(\rho-\nu)}{a}]}{\Gamma[\frac{i\rho}{a}]}, \quad (150)$$

$$\overleftarrow{\beta}_{34}^*(\nu, \rho) = -\frac{1}{2\pi a} \sqrt{\frac{\nu}{\rho}} \frac{2^{\frac{i(\rho+\nu)}{a}} \Gamma[\frac{i\nu}{a}] \Gamma[\frac{-i(\rho+\nu)}{a}]}{\Gamma[\frac{-i\rho}{a}]}, \quad (151)$$

From the definition:

$$|\overleftarrow{\beta}_{34}(\nu, \rho)|^2 = \overleftarrow{\beta}_{34}^*(\nu, \rho) \overleftarrow{\beta}_{34}(\nu, \rho), \quad (152)$$

Substituting Eq. (151) into Eq. (152), we obtain:

$$|\overleftarrow{\beta}_{34}(\nu, \rho)|^2 = \frac{1}{4\pi^2 a^2} \frac{\nu}{\rho} \frac{|\Gamma[\frac{i\nu}{a}]|^2 |\Gamma[\frac{i(\nu+\rho)}{a}]|^2}{|\Gamma[\frac{i\rho}{a}]|^2}, \quad (153)$$

Simplifying the above expression using properties of the Gamma function yields:

$$|\overleftarrow{\beta}_{34}(\nu, \rho)|^2 = \frac{1}{4\pi a} \frac{\sinh(\frac{\pi\rho}{a})}{(\nu + \rho) \sinh(\frac{\pi\nu}{a}) \sinh[\frac{\pi(\nu+\rho)}{a}]}, \quad (154)$$

Since R_4 is obtained through a null shift from R_1 , the resulting quantum field configuration exhibits selective thermalisation, and the right-moving modes become thermally populated. In contrast, the left-moving modes remain in the vacuum, as established earlier. The corresponding quantum state in the region R_4 is a tensor product state in the Hilbert space \mathcal{H}_{R_4} , and is given by[25, 26].

$$|\psi_{R_4}\rangle = \left(\sum_{n=0}^{\infty} \sqrt{p_n} |\vec{n}\rangle \right) \otimes |\overleftarrow{0}\rangle, \quad (155)$$

Where; $p_n = \frac{e^{-n\beta\rho}}{Z}$ is the thermal weight, having partition function $Z = \sum_{n=0}^{\infty} e^{-n\beta\rho}$. Here, $|\vec{n}\rangle$ denotes the n -particle Fock basis state of the right-moving modes, and $|\overleftarrow{0}\rangle$ is the vacuum state for the left-moving modes in R_4 . A detailed discussion of the structure and interpretation of this state—including its relation to thermal density matrices and purification—is provided in Appendix C.

We now compute the expectation value of the number operator for left-moving modes in the region R_3 , to the quantum state in region R_4 . That is:

$$\langle \overleftarrow{\hat{N}}_{34}(\nu) \rangle = \langle \psi_{R_4} | \overleftarrow{\hat{b}}_3^\dagger(\nu) \overleftarrow{\hat{b}}_3(\nu) | \psi_{R_4} \rangle, \quad (156)$$

Substituting the Bogoliubov transformation relations from Eqs. (63) and (64) into Eq. (156) and using the ($j=3$ and $i=4$ and also $\Omega = \nu$ and $\omega = \rho$), we obtain:

$$\langle \overleftarrow{\hat{N}}_{34}(\nu) \rangle = \langle \psi_{R_4} | \int_0^{\infty} d\rho \int_0^{\infty} d\rho' \overleftarrow{\hat{b}}_{34}^*(\nu, \rho) \overleftarrow{\hat{b}}_{34}(\nu, \rho') \overleftarrow{\hat{b}}_4^\dagger(\rho') \overleftarrow{\hat{b}}_4(\rho) | \psi_{R_4} \rangle, \quad (157)$$

To evaluate this expression, recall from Eq. (155) that the state $|\psi_{R_4}\rangle$ is a tensor product with the left-moving mode in the vacuum. Therefore, the two-point function reduces to a vacuum expectation value:

$$\langle \psi_{R_4} | \overleftarrow{\hat{b}}_4(\rho') \overleftarrow{\hat{b}}_4^\dagger(\rho) | \psi_{R_4} \rangle = \langle \overleftarrow{0} | \overleftarrow{\hat{b}}_4(\rho') \overleftarrow{\hat{b}}_4^\dagger(\rho) | \overleftarrow{0} \rangle, \quad (158)$$

Since the left-moving modes are in vacuum in $|\psi_{R_4}\rangle$, we obtain:

$$\langle \overleftarrow{0} | \overleftarrow{\hat{b}}_4(\rho') \overleftarrow{\hat{b}}_4^\dagger(\rho) | \overleftarrow{0} \rangle = \delta(\rho - \rho'), \quad (159)$$

From Eqs. (157)–(159), we obtain

$$\langle \overleftarrow{\hat{N}}_{34}(\nu) \rangle = \int_0^{\infty} d\rho |\overleftarrow{\beta}_{34}(\nu, \rho)|^2, \quad (160)$$

Substituting Eq. (154) into Eq. (160) yields an expression structurally identical to Eq. (81), and we obtain:

$$\langle \overleftarrow{\hat{N}}_{34}(\nu) \rangle = \frac{\delta(0)}{e^{\frac{2\pi\nu}{a}} - 1}, \quad (161)$$

Where the delta function $\delta(0)$ arises due to the normalisation of the continuous frequency modes and indicates

a formally infinite total density per unit frequency. We can therefore identify the mean particle number density per unit frequency ν in the R_3 vacuum as observed in R_4 as:

$$\overleftarrow{n}_{34}(\nu) = \frac{1}{e^{\frac{2\pi\nu}{a}} - 1}, \quad (162)$$

This corresponds to a Planckian spectrum at a temperature of $T = \frac{a}{2\pi}$. Thus, we conclude that the left-moving modes connecting regions R_4 and R_3 are thermally populated with a Planckian distribution, as perceived by observers in R_3 , when the field is selectively excited $|\psi_{R_4}\rangle$.

We now define the state vector in the Rindler region R_3 as observed from the vacuum state in R_1 , following the composite path $R_1 \rightarrow R_4 \rightarrow R_3$ (Path 4). The vacuum in R_1 is defined by:

$$\overrightarrow{a}_1 |0_{R_1}\rangle = 0 \quad \text{and} \quad \overleftarrow{b}_1 |0_{R_1}\rangle = 0, \quad (163)$$

Along this path, the right-moving modes become thermally populated in the transition $R_1 \rightarrow R_4$, and the left-moving modes undergo thermal excitations during the transition $R_4 \rightarrow R_3$.

a. Composing Bogoliubov Coefficients: As in Section C, we compose the Bogoliubov coefficients for the two-step transformation $R_1 \rightarrow R_4 \rightarrow R_3$.

$$\beta_{31}(\nu, \omega) = \int d\rho [\beta_{34}(\nu, \rho) \alpha_{41}(\rho, \omega) - \alpha_{34}(\nu, \rho) \beta_{41}(\rho, \omega)]. \quad (164)$$

This relates the Bogoliubov coefficient between modes in R_3 and R_1 to the intermediate transformations through region R_4 , following the same structure as Eq. (133) in the previous section.

b. Right-Moving mode: In the first leg of the path, $R_1 \rightarrow R_4$, the right-moving modes are thermally excited, while the second leg, $R_4 \rightarrow R_3$, leaves the right-moving modes unchanged. Using Eqs. (142), (143), and Eq (164), we obtain:

$$\overrightarrow{\beta}_{31}(\nu, \omega) = -\overrightarrow{\beta}_{41}(\nu, \omega), \quad (165)$$

Since, $\overrightarrow{\beta}_{41}$ is thermal, it follows that $\overrightarrow{\beta}_{31}$ also exhibits thermal behavior.

c. Left-moving mode: For the left-moving mode, the thermal contribution arises from the transformation $R_4 \rightarrow R_3$, while the transition $R_1 \rightarrow R_4$ leaves the left-moving modes in the vacuum. Therefore,

$$\overleftarrow{\beta}_{31}(\nu, \omega) = \overleftarrow{\beta}_{34}(\nu, \omega), \quad (166)$$

Since $\overleftarrow{\beta}_{34}$ is thermal, this confirms that the left-moving modes in region R_3 also appear excited with thermal weight when viewed from the vacuum in R_1 .

We therefore conclude that, along the path 4 from region R_1 to R_3 , both the left- and right-moving modes undergo Bogoliubov transformations that excite particles relative to the initial vacuum $|0_{R_1}\rangle$. The left-moving

mode acquires thermal excitation through the transition $R_1 \rightarrow R_4$, while the right-moving sector becomes thermal due to the transformation $R_4 \rightarrow R_3$, as demonstrated by Eqs. (165) and (166).

The resulting state in wedge R_3 , as expressed in the number basis of left- and right-moving modes, thus takes the form:

$$|\psi_{R_3}\rangle = \left(\sum_m \sqrt{q_m} |\overleftarrow{m}\rangle \right) \otimes \left(\sum_n \sqrt{p_n} |\overrightarrow{n}\rangle \right), \quad (167)$$

Eq. (167) describes a product of two pure states in the Fock space of region R_3 as in the previous section, each written as a thermal-like superposition over number eigenstates. Although the coefficients p_n and q_m exhibit thermal distributions, the global state is pure and unentangled between the left- and right-moving modes.

This structure is not equivalent to a thermofield double, which would involve entanglement across the two modes. Rather, the thermal character in each mode arises independently due to the composite Bogoliubov transformation along the path $R_1 \rightarrow R_4 \rightarrow R_3$. A detailed discussion of the structure and interpretation of this state is provided in Appendix D.

E. Bogoliubov Transformation for two observes in Rindler spacetime

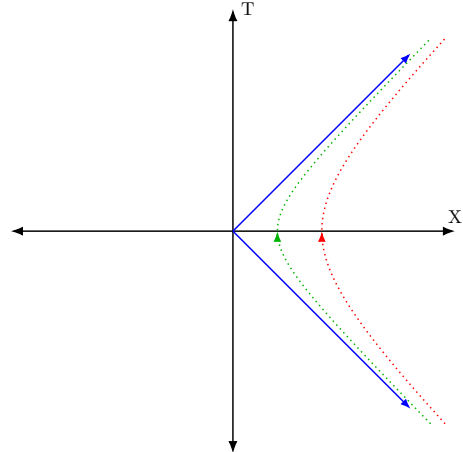


FIG. 3. Rindler spacetime with an observer experiencing acceleration a and g , shown in green and red, respectively.

We now consider the relation between two Rindler observers accelerating with proper accelerations a and g , respectively. The coordinate transformation from Minkowski to Rindler coordinates with acceleration a is given by:

$$T = \frac{e^{ax_1}}{a} \sinh(a t_1), \quad (168)$$

$$X = \frac{e^{a x_1}}{a} \cosh(a t_1). \quad (169)$$

which in light-cone coordinates takes the form:

$$U = T - X = -\frac{e^{-a u_1}}{a}, \quad (170)$$

$$V = T + X = \frac{e^{a v_1}}{a}. \quad (171)$$

Similarly, for Rindler coordinates with acceleration g , we have:

$$T = \frac{e^{g x_2}}{g} \sinh(g t_2), \quad (172)$$

$$X = \frac{e^{g x_2}}{g} \cosh(g t_2), \quad (173)$$

and in light-cone form:

$$U = T - X = -\frac{e^{-g u_2}}{g}, \quad (174)$$

$$V = T + X = \frac{e^{g v_2}}{g}, \quad (175)$$

By equating the light-cone coordinates U and V in the two charts, we find the transformations between the null coordinates:

$$u_1 = \frac{-1}{a} \ln\left(\frac{a}{g}\right) + \frac{g}{a} u_2, \quad (176)$$

$$v_1 = \frac{1}{a} \ln\left(\frac{a}{g}\right) + \frac{g}{a} v_2, \quad (177)$$

Using these relations, we evaluate the Bogoliubov coefficients for right-moving modes via:

$$\overrightarrow{\alpha}^*_{\Omega, \omega} = \frac{1}{2\pi} \sqrt{\frac{\Omega}{\omega}} \int_{-\infty}^{\infty} du_2 e^{i \Omega u_2} e^{-i \omega u_1} \quad (178)$$

$$\overrightarrow{\beta}^*_{\Omega \omega} = -\frac{1}{2\pi} \sqrt{\frac{\Omega}{\omega}} \int_{-\infty}^{\infty} du_2 e^{i \Omega u_2} e^{i \omega u_1}, \quad (179)$$

Substituting Eq. (176) into Eq. (178), we obtain:

$$\overrightarrow{\alpha}^*_{\Omega, \omega} = \frac{1}{2\pi} \sqrt{\frac{\Omega}{\omega}} \left(\frac{a}{g}\right)^{\frac{i\omega}{a}} \int_{-\infty}^{\infty} du_2 e^{i u_2 \left(\Omega - \frac{\omega g}{a}\right)}, \quad (180)$$

By the integration technique, we obtained the following result.

$$\overrightarrow{\alpha}^*_{\Omega, \omega} = \sqrt{\frac{\Omega}{\omega}} \left(\frac{a}{g}\right)^{\frac{i\omega}{a}} \delta\left(\Omega - \frac{\omega g}{a}\right), \quad (181)$$

Similarly, the β^* -coefficient becomes

$$\overrightarrow{\beta}^*_{\Omega, \omega} = -\frac{1}{2\pi} \sqrt{\frac{\Omega}{\omega}} \left(\frac{a}{g}\right)^{\frac{-i\omega}{a}} \int_{-\infty}^{\infty} du_2 e^{i u_2 \left(\Omega + \frac{\omega g}{a}\right)}, \quad (182)$$

Hence, by integrating Eq. (182), we get

$$\overrightarrow{\beta}^*_{\Omega, \omega} = 0, \quad (183)$$

Following a similar analysis for left-moving modes, we obtain:

$$\overleftarrow{\alpha}^*_{\Omega, \omega} = \sqrt{\frac{\Omega}{\omega}} \left(\frac{a}{g}\right)^{\frac{-i\omega}{a}} \delta\left(\Omega - \frac{\omega g}{a}\right), \quad (184)$$

$$\overleftarrow{\beta}^*_{\Omega, \omega} = 0, \quad (185)$$

Thus, both left- and right-moving Bogoliubov coefficients $\beta_{\Omega \omega}$ vanish. This indicates that the Rindler vacuum defined with acceleration a appears as a vacuum to observers accelerating with g , i.e., no particle creation occurs between these frames.

V. CONFORMAL TRANSFORMATIONS AND ENERGY FLUX IN TWO-DIMENSIONAL CONFORMAL FIELD THEORIES

In this section, we investigate the thermal properties of the nested Rindler wedges shown in Figs. 1 and 2 through the expectation values of the energy-momentum tensor in a two-dimensional conformal field theory. Our approach begins with the Minkowski vacuum $|0_M\rangle$, tracing the emergence of thermal behaviour along the alternative paths described in the preceding section. We then repeat the analysis using the Rindler vacuum $|0_{R_1}\rangle$ associated with the wedge R_1 , allowing us to directly contrast the thermal signatures arising from the two different vacuum choices.

A. Two-Dimensional CFT on Rindler Spacetime in the Minkowski Vacuum

To investigate the Minkowski Vacuum $|0_M\rangle$, as perceived by a uniformly accelerated Rindler observer via different paths. We are using the Schwarzian derivative to compute the expectation value of the components of the energy-momentum tensor through the Minkowski Vacuum $|0_M\rangle$. In a 2d CFT on Minkowski spacetime, the energy-momentum tensor satisfies[27]:

$$\partial_\mu T^{\mu\nu} = 0, \quad (186)$$

From the above equation, we have the non-vanishing components are $T_{U_M U_M}$ and $T_{V_M V_M}$. Furthermore, in the Minkowski Vacuum state $|0_M\rangle$,

$$\langle 0_M | T_{U_M U_M} | 0_M \rangle = 0 \quad \langle 0_M | T_{V_M V_M} | 0_M \rangle = 0, \quad (187)$$

And the expectation value of the energy-momentum tensor is defined with respect to the Minkowski Vacuum state $|0_M\rangle$,

$$\langle 0_M | : T_{uu} : |0_M \rangle = -\frac{\hbar}{24\pi} S(U, u), \quad (188)$$

From Eqs. (3), (4), (66) and (188) and after a simple calculation the expectation value of the energy-momentum tensor in Rindler R_1 gives,

$$\langle 0_M | : T_{u_1 u_1} : |0_M \rangle = \frac{\hbar a^2}{48\pi}, \quad (189)$$

$$\langle 0_M | : T_{v_1 v_1} : |0_M \rangle = \frac{\hbar a^2}{48\pi}, \quad (190)$$

Similarly, the the expectation value in R_3 directly with respect to Minkowski Vacuum $|0_M\rangle$ is calculated as:

$$\langle 0_M | : T_{u_3 u_3} : |0_M \rangle = \frac{\hbar a^2}{48\pi}, \quad (191)$$

$$\langle 0_M | : T_{v_3 v_3} : |0_M \rangle = \frac{\hbar a^2}{48\pi}, \quad (192)$$

We than compute the expectation values in R_3 through the excited state R_1 by the following equations[10],

$$\begin{aligned} \langle 0_M | : T_{u_3 u_3} : |0_M \rangle &= \left(\frac{\partial u_1}{\partial u_3} \right)^2 \langle 0_M | : T_{u_1 u_1} : |0_M \rangle \\ &\quad - \frac{\hbar}{24\pi} S(u_1, u_3), \end{aligned} \quad (193)$$

And,

$$\begin{aligned} \langle 0_M | : T_{v_3 v_3} : |0_M \rangle &= \left(\frac{\partial v_1}{\partial v_3} \right)^2 \langle 0_M | : T_{v_1 v_1} : |0_M \rangle \\ &\quad - \frac{\hbar}{24\pi} S(v_1, v_3), \end{aligned} \quad (194)$$

Eqs. (193) and (194) are known as the Virasoro anomaly.

By using Eqs. (9), (66),Eqs. (189) and Eqs. (193), we get the expectation value in R_3 through the excited state R_1 is,

$$\langle 0_M | : T_{u_3 u_3} : |0_M \rangle = \frac{\hbar a^2}{48\pi}, \quad (195)$$

And similarly, using Eqs. (10), (66),Eqs. (190) and Eqs. (194), we get the expectation value in R_3 through the excited state R_1 is,

$$\langle 0_M | : T_{v_3 v_3} : |0_M \rangle = \frac{\hbar a^2}{48\pi}, \quad (196)$$

Now, as the above calculation, the Null shifted wedges R_2 and R_4 through R_1 as shown in Figs. 1 and 2 simply gives,

$$\langle 0_M | : T_{u_2 u_2} : |0_M \rangle = \frac{\hbar a^2}{48\pi} = \langle 0_M | : T_{v_3 v_3} : |0_M \rangle, \quad (197)$$

And

$$\langle 0_M | : T_{u_4 u_4} : |0_M \rangle = \frac{\hbar a^2}{48\pi} = \langle 0_M | : T_{v_4 v_4} : |0_M \rangle, \quad (198)$$

Also, the expectation values in the Rindler wedge R_3 via null-shifted through the Rindler wedges R_2 and R_4 as shown in Figs. 1 and 2 simply gives as above,

$$\langle 0_M | : T_{u_3 u_3} : |0_M \rangle = \frac{\hbar a^2}{48\pi} = \langle 0_M | : T_{v_3 v_3} : |0_M \rangle, \quad (199)$$

Our analysis shows that the Minkowski vacuum, when viewed from any of the Rindler wedges, whether spatially separated or null shifted, exhibits identical expectation values for the chiral components of the energy-momentum tensor. In every case, the Schwarzian derivative associated with the coordinate transformation reproduces the standard thermal stress tensor, reflecting the Unruh temperature perceived by uniformly accelerated observers. We conclude that regardless of whether the transformation between wedges, demonstrating that all these wedges are conformally related to Minkowski spacetime.

B. Two-Dimensional CFT on Rindler Spacetime in the Rindler Vacuum

In this section, we again investigate the expectation values of the energy-momentum tensor in the vacuum state as seen from the Rindler wedge R_1 , evaluated via four paths.

An important conceptual difference arises immediately, unlike the Minkowski vacuum, the Rindler vacuum $|0_{R_1}\rangle$ is not a globally defined Hadamard state on Minkowski spacetime[11]. It is only well-defined within the wedge R_1 and not defined on the Horizon, because it is singular on the Horizon, and it is not invariant under translations, boosts, or null shifts. Consequently, extending $|0_{R_1}\rangle$ into the null-shifted wedges R_2 , R_4 or R_3 is not a symmetry operation of quantum field theory and cannot generically define a consistent state in those regions. This subtlety is crucial for understanding the path dependence that emerges below.

The expectation value of the energy-momentum tensor along Path-1, which maps Minkowski space directly to the Rindler wedge R_3 while bypassing R_1 , has already been derived in the preceding section,as given in Eqs. (191) and (192).

Next, we compute the energy-momentum tensor according to Path-2. In this case, the field is evaluated in R_3 ,but the vacuum state is taken to be that of the Rindler wedge R_1 and is denoted as $|0_{R_1}\rangle$.

From Eqs. (11) and (66), we have

$$S(u_1, u_3) = -\frac{a^2 e^{au_3}}{2(1 + e^{au_3})^2} (2 + e^{au_3}), \quad (200)$$

We than compute the expectation values in R_3 through the Vacuum state R_1 by the following equations,

$$\begin{aligned} \langle 0_{R_1} | : T_{u_3 u_3} : | 0_{R_1} \rangle &= \left(\frac{\partial_{u_1}}{\partial_{u_3}} \right)^2 \langle 0_{R_1} | : T_{u_1 u_1} : | 0_{R_1} \rangle \\ &\quad - \frac{\hbar}{24\pi} S(u_1, u_3), \end{aligned} \quad (201)$$

In the Rindler Vacuum state R_1 ,

$$\langle 0_{R_1} | : T_{u_1 u_1} : | 0_{R_1} \rangle = \langle 0_{R_1} | : T_{v_3 v_3} : | 0_{R_1} \rangle = 0, \quad (202)$$

From Eqs. (200), (201) and (202), we obtain:

$$\langle 0_{R_1} | : T_{u_3 u_3} : | 0_{R_1} \rangle = \frac{\hbar a^2 e^{au_3} (2 + e^{au_3})}{48\pi (1 + e^{au_3})^2}, \quad (203)$$

Eq. (203) can be evaluated for different limits.

a. $u_3 \rightarrow 0$

$$\langle 0_{R_1} | : T_{u_3 u_3} : | 0_{R_1} \rangle = \frac{\hbar a^2}{64\pi}$$

b. $u_3 \rightarrow \infty$

$$\langle 0_{R_1} | : T_{u_3 u_3} : | 0_{R_1} \rangle = \frac{\hbar a^2}{48\pi}$$

c. $u_3 \rightarrow -\infty$

$$\langle 0_{R_1} | : T_{u_3 u_3} : | 0_{R_1} \rangle = 0$$

Similarly we can calculate,

$$\langle 0_{R_1} | : T_{v_3 v_3} : | 0_{R_1} \rangle = \frac{\hbar a^2 (1 + 2e^{av_3})}{48\pi (1 + e^{av_3})^2}, \quad (204)$$

Eq. (204) can be evaluated for different limits as above.

d. $v_3 \rightarrow 0$

$$\langle 0_{R_1} | : T_{v_3 v_3} : | 0_{R_1} \rangle = \frac{\hbar a^2}{64\pi}$$

e. $v_3 \rightarrow \infty$

$$\langle 0_{R_1} | : T_{v_3 v_3} : | 0_{R_1} \rangle = \frac{\hbar a^2}{24\pi} e^{-av_3}$$

f. $v_3 \rightarrow -\infty$

$$\langle 0_{R_1} | : T_{v_3 v_3} : | 0_{R_1} \rangle = \frac{\hbar a^2}{48\pi}$$

Now, we are evaluating the expectation values of energy-momentum tensor in the null-shifted wedge R_2 as shown in Fig. 1 with respect to vacuum state in R_1 . From Eqs. (17) and (66), we get

$$S(u_1, u_2) = 0, \quad (205)$$

A simple calculation, gives

$$\langle 0_{R_1} | : T_{u_2 u_2} : | 0_{R_1} \rangle = 0, \quad (206)$$

And similarly we can calculate,

$$\langle 0_{R_1} | : T_{v_2 v_2} : | 0_{R_1} \rangle = \frac{\hbar a^2 (1 + 2e^{av_2})}{48\pi (1 + e^{av_2})^2}, \quad (207)$$

Eq. (207) can be evaluated for different limits as above.

g. $v_2 \rightarrow 0$

$$\langle 0_{R_1} | : T_{v_2 v_2} : | 0_{R_1} \rangle = \frac{\hbar a^2}{64\pi}$$

h. $v_2 \rightarrow \infty$

$$\langle 0_{R_1} | : T_{v_2 v_2} : | 0_{R_1} \rangle = \frac{\hbar a^2}{24\pi} e^{-av_2}$$

i. $v_2 \rightarrow -\infty$

$$\langle 0_{R_1} | : T_{v_2 v_2} : | 0_{R_1} \rangle = \frac{\hbar a^2}{48\pi}$$

In the above discussion we observe that with respect to Rindler vacuum state R_1 the component of the $T_{u_2 u_2}$ is zero and $T_{v_2 v_2}$ is non-zero as discussed above.

Now we evaluate the expectation values of the energy-momentum tensor in the Rindler wedge R_3 via Path-3, using the Rindler vacuum defined in R_1 , the expectation value of energy-momentum tensor is

$$\begin{aligned} \langle 0_{R_1} | : T_{u_3 u_3} : | 0_{R_1} \rangle &= \left(\frac{\partial_{u_1}}{\partial_{u_3}} \right)^2 \langle 0_{R_1} | : T_{u_2 u_2} : | 0_{R_1} \rangle \\ &\quad - \frac{\hbar}{24\pi} S(u_1, u_3), \end{aligned} \quad (208)$$

And,

$$\begin{aligned} \langle 0_{R_1} | : T_{v_3 v_3} : | 0_{R_1} \rangle &= \left(\frac{\partial_{v_1}}{\partial_{v_3}} \right)^2 \langle 0_{R_1} | : T_{v_2 v_2} : | 0_{R_1} \rangle \\ &\quad - \frac{\hbar}{24\pi} S(v_1, v_3), \end{aligned} \quad (209)$$

From Eqs. (200), (206) and (208), we get

$$\langle 0_{R_1} | : T_{u_3 u_3} : | 0_{R_1} \rangle = \frac{\hbar a^2 e^{au_3} (2 + e^{au_3})}{48\pi (1 + e^{au_3})^2}, \quad (210)$$

Eq. (210) is exactly match with the Eq. (203) and hence gives the same limiting condition. Similarly, by the simple calculations, we get

$$\langle 0_{R_1} | : T_{v_3 v_3} : | 0_{R_1} \rangle = \frac{\hbar a^2}{48\pi} \frac{(2e^{av_3} + 1)}{(e^{av_3} + 1)^4} (2e^{2av_3} + 2e^{av_3} + 1), \quad (211)$$

Eq. (211) can be evaluated for different limits as above.

j. $v_3 \rightarrow 0$

$$\langle 0_{R_1} | : T_{v_3 v_3} : | 0_{R_1} \rangle = \frac{5\hbar a^2}{256\pi}$$

k. $v_3 \rightarrow \infty$

$$\langle 0_{R_1} | : T_{v_3 v_3} : | 0_{R_1} \rangle = \frac{\hbar a^2}{12\pi} e^{-av_3}$$

l. $v_3 \rightarrow -\infty$

$$\langle 0_{R_1} | : T_{v_3 v_3} : | 0_{R_1} \rangle = \frac{\hbar a^2}{48\pi}$$

Finally, we evaluate the expectation values of the energy-momentum tensor in the Rindler wedge R_3 along Path-4 as in the above calculations. In this path, the field configuration is mapped according to $R_1 \rightarrow R_4 \rightarrow R_3$, where the intermediate wedge R_4 plays the role opposite to that of R_2 in Path-3. Specifically, while in R_2 we found $\langle T_{u_2 u_2} \rangle = 0$ and a nonvanishing $\langle T_{v_2 v_2} \rangle$, the corresponding expectation values in R_4 are simply interchanged, with $\langle T_{v_4 v_4} \rangle = 0$ and $\langle T_{u_4 u_4} \rangle$ taking the same functional form as $\langle T_{v_2 v_2} \rangle$. When this R_4 is propagated into R_3 , the derivative factors and Schwarzian contributions appearing in the $R_4 \rightarrow R_3$ transformation reproduce the same expressions as those obtained along Path-3. As a result, the final expectation value of the stress-energy components, $\langle 0_{R_1} | : T_{u_3 u_3} : | 0_{R_1} \rangle$, $\langle 0_{R_1} | : T_{v_3 v_3} : | 0_{R_1} \rangle$, computed via Path-4 coincide identically with the corresponding components derived along Path-3. This confirms that both paths lead to the same stress-energy tensor in R_3 , demonstrating the internal consistency and path independence of the setup.

Taken together with the results of Sec. V A, our analysis reveals a clear structural distinction between the two vacuum choices. For the Minkowski vacuum $|0_M\rangle$, all four paths connecting the nested Rindler wedges yield the same thermal expectation values in R_3 , reflecting the conformal equivalence of the wedges and the universality of the Unruh temperature. In contrast, when the Rindler vacuum $|0_{R_1}\rangle$ is used, the four paths no longer agree; Path-1 and Path-2 produce distinct stress-tensor components in R_3 , while Path-3 and Path-4 agree with each other but differ from Paths 1 and 2. This demonstrates that, unlike the Minkowski vacuum, the Rindler vacuum is sensitive to the choice of intermediate wedge, reflecting its non-invariance under the full modular flow connecting the nested Rindler regions.

The above comparison also highlights an essential physical distinction between the two vacuum choices. When the Minkowski vacuum $|0_M\rangle$ is used, all paths consistently reproduce the standard thermal stress tensor associated with the Unruh effect. This reflects a genuinely physical thermality; a uniformly accelerated observer perceives the Minkowski vacuum as a thermal state at the Unruh temperature, in complete agreement with quantum field theory in curved spacetime. In contrast, when the Rindler vacuum $|0_{R_1}\rangle$ is employed, the resulting stress-tensor components display path dependence and fail to yield a universal thermal spectrum. The apparent thermality that emerges in this case is therefore not physical but merely an effective or coordinate-induced thermality, arising from the restricted domain of the Rindler vacuum rather than from any true thermal bath. Thus, the Minkowski vacuum leads to genuine Unruh thermality, while the Rindler vacuum generates only a formal, non-physical analogue.

VI. CONCLUSION

We have investigated the emergence of thermal behaviour in two-dimensional Rindler spacetime by analysing a hierarchy of spatially shifted and null-shifted wedge constructions in Minkowski space. By combining Bogoliubov transformations with an independent evaluation of the expectation value of the stress-energy tensor, we have shown that thermal occupation numbers, Gibbs thermality, and entanglement across horizons are logically distinct features whose relation depends sensitively on the underlying geometry and choice of vacuum.

Uniformly accelerated observers associated with different Rindler wedges and characterised by distinct accelerations a and g do not, in general, detect particles with respect to each other's natural vacuum states. This result demonstrates that relative acceleration alone is insufficient to generate particle production or thermality, and that the Unruh effect relies crucially on the presence of a causal horizon and the accompanying entanglement structure of the Minkowski vacuum.

When the global state is the Minkowski vacuum, thermal occupation numbers detected in a single Rindler wedge arise from tracing over degrees of freedom beyond the horizon. The resulting local state is mixed and Gibbsian, with both left- and right-moving sectors exhibiting thermal occupation. In contrast, null-shifted wedge constructions give rise to thermal occupation numbers in the absence of entanglement between complementary wedges. In these cases, the global and local quantum states remain pure, and thermal behaviour emerges solely from Bogoliubov mixing induced by null translations along Rindler horizons. The thermality is therefore selective, affecting only one chiral sector while the complementary sector remains in its vacuum.

The stress-energy tensor provides an independent and physically robust diagnostic of these distinctions. When evaluated in the Minkowski vacuum, its expectation value is universal and insensitive to the particular sequence of wedge constructions, reflecting genuine horizon-induced thermality. By contrast, when evaluated in the Rindler vacuum, the stress-energy tensor exhibits path-dependent and unphysical behaviour, underscoring that apparent thermal occupation numbers alone do not guarantee a physically meaningful thermal state.

Taken together, these results demonstrate the existence of inequivalent purifications of thermal occupation numbers in Rindler spacetime. They establish explicitly that thermal behaviour need not originate from entanglement or mixedness of the quantum state. In this sense, the null-shifted constructions realise a converse perspective on the Unruh effect, in which thermal occupation arises from kinematical mode mixing rather than from tracing over inaccessible degrees of freedom. More broadly, our findings clarify the distinct roles of observer dependence, causal structure, and vacuum choice in the emergence of thermality in relativistic quantum field theory.

Appendix A: Calculation of Bogoliubov coefficient

Bogoliubov coefficient $\alpha_{21}^*(\Omega\omega)$ is written as

$$\alpha_{21}^*(\Omega, \omega) = \frac{1}{2\pi} \sqrt{\frac{\Omega}{\omega}} \int_{-\infty}^{\infty} dv_2 e^{i\Omega v_2} e^{-i\omega v_1} \quad (\text{A1})$$

Substituting Eq. (22) in the (A1), we have

$$\alpha_{21}^*(\Omega, \omega) = \frac{1}{2\pi} \sqrt{\frac{\Omega}{\omega}} \int_{-\infty}^{\infty} dv_2 e^{i\Omega v_2} e^{\frac{-i\omega \ln[e^a v_2 + 1]}{a}} \quad (\text{A2})$$

Hence, (A2) can be written as

$$\alpha_{21}^*(\Omega, \omega) = \frac{1}{2\pi} \sqrt{\frac{\Omega}{\omega}} \int_{-\infty}^{\infty} dv_2 e^{i\Omega v_2} (e^{a v_2} + 1)^{-\frac{i\omega}{a}} \quad (\text{A3})$$

By substituting $e^{a v_2} + 1 = h \implies h - 1 = e^{a v_2}$ and also $dv_2 = \frac{dh}{a(h-1)}$ in the above equation. Hence (A3) reduces to,

$$\alpha_{21}^*(\Omega, \omega) = \frac{1}{2\pi} \sqrt{\frac{\Omega}{\omega}} \int_{2a\Delta_1}^{\infty} dh (h-1)^{\frac{i\Omega}{a}-1} h^{-\frac{i\omega}{a}} \quad (\text{A4})$$

Again, substituting $h - 2a\Delta_1 = t \implies h = t + 2a\Delta_1$ and also $dh = dt$ in (A4) and hence we can write,

$$\alpha_{21}^*(\Omega, \omega) = \frac{1}{2\pi a} \sqrt{\frac{\Omega}{\omega}} \int_0^{\infty} dt t^{\frac{i\Omega}{a}-1} (t+1)^{-\frac{i\omega}{a}} \quad (\text{A5})$$

The integral in (A5) can be evaluated from Mathematica and therefore can be written as

$$\alpha_{21}^*(\Omega, \omega) = \frac{1}{2\pi a} \sqrt{\frac{\Omega}{\omega}} \frac{2^{\frac{-i\omega+i\Omega}{a}} \Gamma[\frac{i\Omega}{a}] \Gamma[\frac{i\omega-i\Omega}{a}]}{\Gamma[\frac{i\omega}{a}]} \quad (\text{A6})$$

From Eq. (75), Bogoliubov coefficient $\beta_{21}^*(\Omega\omega)$ is written as

$$\beta_{21}^*(\Omega, \omega) = -\frac{1}{2\pi} \sqrt{\frac{\Omega}{\omega}} \int_{-\infty}^{\infty} dv_2 e^{i\Omega v_2} e^{i\omega v_1} \quad (\text{A7})$$

As the above calculation (A7) can be written as

$$\beta_{21}^*(\Omega, \omega) = -\frac{1}{2\pi a} \sqrt{\frac{\Omega}{\omega}} \int_0^{\infty} dt t^{\frac{i\Omega}{a}-1} (t+1)^{\frac{i\omega}{a}} \quad (\text{A8})$$

By the integration technique (A8) can be written as

$$\beta_{21}^*(\Omega'\omega) = -\frac{1}{2\pi a} \sqrt{\frac{\Omega}{\omega}} \frac{2^{\frac{i(\omega+\Omega)}{a}} \Gamma[\frac{i\Omega}{a}] \Gamma[\frac{-i(\omega+\Omega)}{a}]}{\Gamma[\frac{-i\omega}{a}]}, \quad (\text{A9})$$

Appendix B: Particle number density

We solve the integral (92) in this appendix. Let;

$$I = \int_0^{\infty} d\Omega \frac{\sinh(\frac{\pi\Omega}{a})}{(\nu + \Omega) \sinh[\frac{\pi(\nu+\Omega)}{a}]}, \quad (\text{B1})$$

Let; $\frac{(\nu+\Omega)}{a} = z \implies \frac{\pi\Omega}{a} = z - \frac{\pi\nu}{a}$, Also; $d\Omega = \frac{a dz}{\pi}$
Substituting these values in the Integral (B1), we obtain,

$$I = \int_{\frac{\pi\nu}{a}}^{\infty} \frac{dz}{z} \frac{\sinh(z - \frac{\pi\nu}{a})}{\sinh z}, \quad (\text{B2})$$

After some algebra, The Integral (B2) can be written as

$$I = \int_{\frac{\pi\nu}{a}}^{\infty} \frac{dz}{z} [\cosh(\frac{\pi\nu}{a}) - \coth z \sinh(\frac{\pi\nu}{a})], \quad (\text{B3})$$

By substituting The Integral (B3) into Eq. (82), we get

$$\langle \hat{N}(\nu) \rangle = \frac{\cosh(\frac{\pi\nu}{a})}{4\pi a \sinh(\frac{\pi\nu}{a})} \int_{\frac{\pi\nu}{a}}^{\infty} \frac{dz}{z} - \frac{1}{4\pi a} \int_{\frac{\pi\nu}{a}}^{\infty} \frac{dz}{z} \coth z, \quad (\text{B4})$$

Eq. (B4) further split into two integrals,

$$\langle \hat{N}(\nu) \rangle = I_1 - I_2, \quad (\text{B5})$$

Here;

$$I_1 = \frac{\cosh(\frac{\pi\nu}{a})}{2 \sinh(\frac{\pi\nu}{a})} \int_{\frac{\pi\nu}{a}}^{\infty} \frac{1}{2\pi a} \frac{dz}{z}, \quad (\text{B6})$$

The left-hand side of Eq. (B5) gives the dimensionless number of particles. So, I_1 and I_2 must also be dimensionless. To keep the units consistent in Eq. (B6), the factor $\frac{1}{2\pi a}$ is included inside the integral. The integral $\int_{\frac{\pi\nu}{a}}^{\infty} \frac{1}{2\pi a} \frac{dz}{z}$ exhibits a logarithmic ultraviolet (UV) divergence arising from contributions of high-frequency modes. This type of divergence is characteristic of quantum field theories in curved spacetime and often reflects the accumulation of an infinite density of states near horizons or boundaries. In such contexts, divergences are frequently formalized via expressions like $\delta(0)$ —interpreted as an infinite volume or mode density. $\delta(0)$ emerges from continuous mode normalization and is directly linked to spatial volume [28, Sec.2.3]. So the Integral (B6) can be written after simplification;

$$I_1 = \frac{1}{2} \frac{e^{\frac{2\pi\nu}{a}}}{e^{\frac{2\pi\nu}{a}} - 1} \delta(0) + \frac{1}{2} \frac{1}{e^{\frac{2\pi\nu}{a}} - 1} \delta(0), \quad (\text{B7})$$

Now;

$$I_2 = \frac{1}{4\pi a} \int_{\frac{\pi\nu}{a}}^{\infty} \frac{dz}{z} \coth z, \quad (\text{B8})$$

The integral (B8) has a simple pole at $z = n\pi i$ and also a singularity at $z = 0$, as shown in the contour of Fig. 4

By the expansion of $\coth z$,

$$\coth z = \frac{1}{z} + \frac{z}{3} - \frac{z^3}{45} + \dots$$

Explicitly stretching the contour in Fig. 4 by $R \rightarrow \infty$ to $R \rightarrow -\infty$. Now, by the expansion of $\coth z$ at the pole,

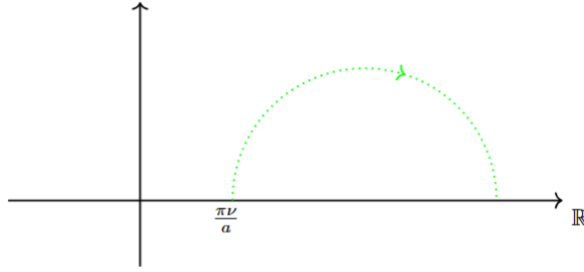


FIG. 4. Complex plane

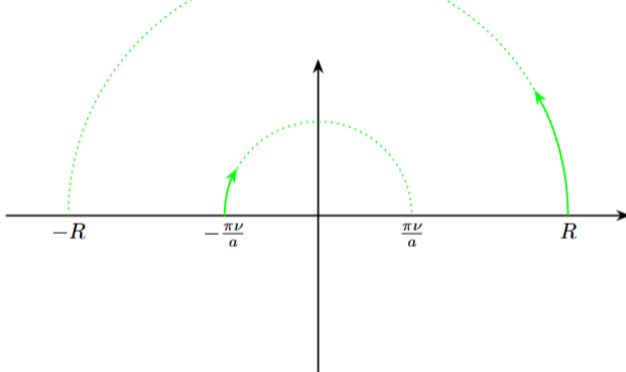


FIG. 5. Complex plane

$$z = n \pi i,$$

$$\coth z = \frac{1}{z - n \pi i} + \text{Reg.part}, \quad (\text{B9})$$

Hence, the residue is

$$\begin{aligned} \text{Residue} &= \lim_{z \rightarrow n \pi i} (z - n \pi i) \frac{\coth z}{z} = \lim_{z \rightarrow n \pi i} \frac{1}{z} \\ &= \frac{1}{n \pi i} \end{aligned}$$

Since; $\frac{1}{\pi i} \sum_{n=1}^{\infty} \frac{1}{n}$ Now;

$$\sum_{n=1}^{\infty} \frac{1}{n} = 1 + \frac{1}{2} + \frac{1}{3} + \frac{1}{4} + \dots = \infty, \quad (\text{B10})$$

Applying the Residue Theorem to a contour, as shown in Fig. 5,

$$\begin{aligned} &\int_{-R}^{-\frac{\pi \nu}{a}} f(z) dz + \int_{-\frac{\pi \nu}{a}}^R f(z) dz + \int_0^\pi f(R e^{i\theta}) i R e^{i\theta} d\theta + \\ &\int_\pi^0 f\left(\frac{\pi \nu}{a} e^{i\theta}\right) i \frac{\pi \nu}{a} e^{i\theta} d\theta = 2\pi i \left(\frac{1}{\pi i}\right)(\infty), \end{aligned} \quad (\text{B11})$$

Where; $f(z) = \frac{1}{z} \coth z$ By taking the limit $R \rightarrow \infty$ and

after further simplification of Eq. (B11) reduces to be;

$$2 \int_{\frac{\pi \nu}{a}}^{\infty} \frac{1}{z} \coth z dz + i \int_{\pi}^0 \frac{\pi \nu}{a} \coth\left(\frac{\pi \nu}{a} e^{i\theta}\right) d\theta = \infty, \quad (\text{B12})$$

Since; $i \int_{\pi}^0 \frac{\pi \nu}{a} \coth\left(\frac{\pi \nu}{a} e^{i\theta}\right) d\theta = -i \frac{\pi^2 \nu}{a} \cot h\left(\frac{\pi \nu}{a} e^{i\theta}\right)$, which has a finite value. Hence, (B12) reduced to be,

$$\int_{\frac{\pi \nu}{a}}^{\infty} \frac{1}{z} \coth z dz = \infty, \quad (\text{B13})$$

In quantum field theory, integrals that reduce to infinity due to a simple pole can be interpreted in a distributional sense as Dirac delta functions[29–31]. Hence, Eq. (B13) can be written as

$$\int_{\frac{\pi \nu}{a}}^{\infty} \frac{1}{2 \pi a z} \coth z dz = \delta(0), \quad (\text{B14})$$

To maintain dimensional consistency, the factor $\frac{1}{2\pi a}$ is included in the integral. So, from Eq. (B8) and Eq. (B14),

$$I_2 = \frac{1}{2} \delta(0), \quad (\text{B15})$$

Substituting (B7) and (B15) into (B5) and after some algebra, we obtain

$$\langle \hat{N}(\nu) \rangle = \frac{\delta(0)}{e^{\frac{2\pi\nu}{a}} - 1}, \quad (\text{B16})$$

Which has the same functional form as the Bose–Einstein factor, with $\delta(0)$ interpreted as the formal infinite spatial volume factor.

Appendix C: Purity of the State in Region R_2

In this appendix, we verify that the quantum state defined in region R_2 ,

$$|\psi_{R_2}\rangle = \left(\sum_{n=0}^{\infty} \sqrt{p_n} |\vec{n}\rangle \right) \otimes |\vec{0}\rangle, \quad (\text{C1})$$

is a pure state, using the standard formalism of density matrices. Here, the coefficients p_n take the Planckian form

$$p_n = \frac{e^{-n\beta\Omega}}{Z}, \quad Z = \sum_{n=0}^{\infty} e^{-n\beta\Omega}, \quad (\text{C2})$$

and satisfy $\sum_n p_n = 1$.

While these coefficients resemble thermal Boltzmann factors, in this context, they originate from the Bogoliubov amplitudes describing the mode mixing between the vacua of two Rindler-like regions R_1 and R_2 connected

by a null translation. This transformation induces Bogoliubov coefficients whose magnitudes follow a thermal distribution. However, the resultant quantum state in the Hilbert space of R_2 remains a pure vector rather than a mixed state, since the transformation is unitary and no information is lost.

The corresponding density matrix is

$$\rho = |\psi_{R_2}\rangle\langle\psi_{R_2}| = \sum_{n,m} \sqrt{p_n p_m} |\overleftarrow{n}\rangle\langle\overleftarrow{m}| \otimes |\overrightarrow{0}\rangle\langle\overrightarrow{0}|. \quad (\text{C3})$$

This operator is a rank-one projector satisfying $\rho^2 = \rho$. Hence, the state has unit purity,

$$\text{Tr}(\rho^2) = 1, \quad (\text{C4})$$

and is therefore pure.

To isolate the left-moving sector, we trace over the right-moving vacuum:

$$\begin{aligned} \overleftarrow{\rho} &= \text{Tr}_{\overrightarrow{\mathcal{H}}}(\rho) \\ &= \sum_{n,m} \sqrt{p_n p_m} |\overleftarrow{n}\rangle\langle\overleftarrow{m}| \text{Tr}(|\overrightarrow{0}\rangle\langle\overrightarrow{0}|) \\ &= \sum_{n,m} \sqrt{p_n p_m} |\overleftarrow{n}\rangle\langle\overleftarrow{m}|. \end{aligned} \quad (\text{C5})$$

This is again a rank-one operator and can be written as

$$\overleftarrow{\rho} = |\overleftarrow{\psi}\rangle\langle\overleftarrow{\psi}|, \quad |\overleftarrow{\psi}\rangle = \sum_n \sqrt{p_n} |\overleftarrow{n}\rangle. \quad (\text{C6})$$

Therefore,

$$\text{Tr}(\overleftarrow{\rho}^2) = \langle\overleftarrow{\psi}|\overleftarrow{\psi}\rangle = 1, \quad (\text{C7})$$

confirming that the reduced state $\overleftarrow{\rho}$ is also pure.

Although the coefficients p_n exhibit the form of a thermal distribution, they do not represent classical statistical probabilities obtained by tracing out inaccessible degrees of freedom, as is typical for a thermal or Kubo-Martin-Schwinger (KMS) state. Rather, these coefficients arise from the Bogoliubov transformation, which relates mode bases adapted to distinct regions or observers. The squared Bogoliubov coefficients give rise to this thermal-like occupation pattern. It is important to emphasise that the state constructed above is a pure state on the single-wedge algebra, since both chiral sectors appearing in the mode expansion are supported within the same Rindler wedge. No causally complementary algebra is available with respect to which a partial trace could be defined. Consequently, although one chiral sector exhibits a thermal occupation number distribution, the global state remains pure and does not correspond to a thermal density matrix.

Importantly, since no information is lost in this process and the complementary chiral sector remains in its vacuum state, the overall quantum state remains pure.

Thus, while the p_n serve as thermal weights, they fundamentally encode quantum amplitudes within a coherent pure state, rather than reflecting classical probabilistic mixtures.

$$|\psi_{R_2}\rangle = |\overleftarrow{\psi}\rangle \otimes |\overrightarrow{0}\rangle, \quad (\text{C8})$$

With all apparent ‘‘thermality’’ being a kinematic feature of the mode decomposition, not a sign of mixedness or entanglement.

Appendix D: Purity of the State in Region R_3 via Path 3

In this appendix, we analyse the density matrix corresponding to the quantum state in region R_3 , obtained along *Path 3*. Along this path, the left-moving modes acquire Bogoliubov thermal structure during the transition $R_1 \rightarrow R_2$, and the right-moving modes become thermally excited during the subsequent shift $R_2 \rightarrow R_3$. The resulting state in R_3 takes the form

$$|\psi_{R_3}\rangle = \left(\sum_{n=0}^{\infty} \sqrt{p_n} |\overleftarrow{n}\rangle \right) \otimes \left(\sum_{m=0}^{\infty} \sqrt{q_m} |\overrightarrow{m}\rangle \right), \quad (\text{D1})$$

where the coefficients have a Planckian dependence,

$$p_n = \frac{e^{-n\beta\Omega}}{Z}, \quad q_m = \frac{e^{-m\beta\Omega}}{Z}, \quad Z = \sum_{k=0}^{\infty} e^{-k\beta\Omega}.$$

Although these factors resemble thermal Boltzmann weights, in this context, they originate from Bogoliubov amplitudes associated with mode mixing under successive null translations. Their apparent thermality is kinematic, not statistical.

The state $|\psi_{R_3}\rangle$ is a normalized product vector in the Hilbert space \mathcal{H}_{R_3} , and is therefore manifestly pure. The corresponding total density matrix is

$$\begin{aligned} \rho_{R_3} &= |\psi_{R_3}\rangle\langle\psi_{R_3}| \\ &= \sum_{n,m,n',m'=0}^{\infty} \sqrt{p_n p_{n'}} \sqrt{q_m q_{m'}} |\overleftarrow{n}\rangle\langle\overleftarrow{n'}| \otimes |\overrightarrow{m}\rangle\langle\overrightarrow{m'}|. \end{aligned} \quad (\text{D2})$$

This operator is a rank-one projector, satisfying $\rho_{R_3}^2 = \rho_{R_3}$ and $\text{Tr}(\rho_{R_3}) = 1$, which confirms that the global state is pure.

To examine the individual chiral sectors, we trace over one mode. Since the total state is separable, the reduced density matrix of the left-moving mode is

$$\begin{aligned} \overleftarrow{\rho} &= \text{Tr}_{\overrightarrow{\mathcal{H}}}(\rho_{R_3}) \\ &= \left(\sum_{n=0}^{\infty} \sqrt{p_n} |\overleftarrow{n}\rangle \right) \left(\sum_{n'=0}^{\infty} \sqrt{p_{n'}} \langle\overleftarrow{n'}| \right) = |\overleftarrow{\phi}\rangle\langle\overleftarrow{\phi}|, \end{aligned} \quad (\text{D3})$$

where $|\overleftarrow{\phi}\rangle = \sum_n \sqrt{p_n} |\overleftarrow{n}\rangle$. Thus, $\overleftarrow{\rho}$ is a rank-one projector and represents a pure state.

Similarly, tracing over the left-moving sector gives

$$\overrightarrow{\rho} = \text{Tr}_{\overleftarrow{\mathcal{H}}}(\rho_{R_3}) = |\overrightarrow{\phi}\rangle\langle\overrightarrow{\phi}|, \quad |\overrightarrow{\phi}\rangle = \sum_m \sqrt{q_m} |\overrightarrow{m}\rangle. \quad (\text{D4})$$

Both reduced states are pure and separable, confirming that the total state is unentangled.

Although the number-basis coefficients in each sector exhibit thermal-like distributions, the reduced density matrices are rank-one projectors and therefore not thermal in the Gibbs sense [32]. Importantly, this structure

is not a thermofield double (TFD); no entanglement is present between the two chiral sectors. Instead, Eq. (D1) represents an unentangled superposition of number states with Bogoliubov-induced thermal profiles in each mode sector. The apparent thermality emerges purely from independent Bogoliubov mode mixing along Path 3, not from tracing over complementary horizons.

ACKNOWLEDGMENTS

The authors thank the BITS Pilani Hyderabad campus for providing the required infrastructure for this research work.

[1] W. G. Unruh, *Phys. Rev. D* **14**, 870 (1976).

[2] R. Longo, Y. Tanimoto, and Y. Ueda, *Annales Inst. Fourier* **69**, 1229 (2019), arXiv:1706.06070 [math-ph].

[3] S. W. Hawking, *Commun. Math. Phys.* **43**, 199 (1975), [Erratum: Commun.Math.Phys. 46, 206 (1976)].

[4] H. W. Wiesbrock, *Commun. Math. Phys.* **157**, 83 (1993), [Erratum: Commun.Math.Phys. 184, 683–685 (1997)].

[5] L. Aalsma, M. Parikh, and J. P. Van Der Schaar, *JHEP* **11**, 136, arXiv:1905.02714 [hep-th].

[6] S. Gutti, A. U. Nair, and P. Samantray, *Phys. Rev. D* **108**, 025010 (2023), arXiv:2210.08925 [hep-th].

[7] W. Rindler, *Phys. Rev.* **119**, 2082 (1960).

[8] R. M. Wald, *General Relativity* (Chicago Univ. Pr., Chicago, USA, 1984).

[9] E. Frodden and N. Valdés, *Int. J. Mod. Phys. A* **33**, 1830026 (2018), arXiv:1806.11157 [gr-qc].

[10] A. Fabbri and J. Navarro-Salas, *Modeling black hole evaporation* (Cambridge University Press, 2005).

[11] L. Sriramkumar and T. Padmanabhan, *Int. J. Mod. Phys. D* **11**, 1 (2002), arXiv:gr-qc/9903054.

[12] N. D. Birrell and P. C. W. Davies, *Quantum Fields in Curved Space*, Cambridge Monographs on Mathematical Physics (Cambridge University Press, Cambridge, UK, 1982).

[13] R. M. Wald, *Phys. Rev. D* **48**, R2377 (1993).

[14] W. G. Unruh and R. M. Wald, *Phys. Rev. D* **29**, 1047 (1984).

[15] R. Utiyama and B. S. DeWitt, *Journal of Mathematical Physics* **3**, 608 (1962).

[16] R. Blumenhagen and E. Plauschinn, *Introduction to conformal field theory: with applications to String theory*, Vol. 779 (springer, 2009).

[17] V. Mukhanov and S. Winitzki, *Introduction to quantum effects in gravity* (Cambridge University Press, 2007).

[18] R. Haag, *Local quantum physics: Fields, particles, algebras* (Springer, 1992).

[19] T. Padmanabhan, *J. Phys. Conf. Ser.* **306**, 012001 (2011), arXiv:1012.4476 [gr-qc].

[20] S. Kolekar and T. Padmanabhan, *Phys. Rev. D* **89**, 064055 (2014), arXiv:1309.4424 [gr-qc].

[21] T. Padmanabhan, *Gravitation: Foundations and frontiers* (Cambridge University Press, 2014).

[22] J. I. Kapusta and C. Gale, *Finite-Temperature Field Theory: Principles and Applications*, 2nd ed. (Cambridge University Press, Cambridge, UK, 2006) see Chapter 1 (Sections 1.4–1.5) for canonical ensemble and bosonic mode distributions.

[23] R. K. Pathria and P. D. Beale, *Statistical Mechanics*, 3rd ed. (Elsevier, Oxford, 2011) see Chapter 7: Canonical Ensemble; derivation of partition functions and thermal occupation numbers.

[24] F. Anza, *Pure States in Statistical Mechanics: On Its Foundations and Applications to Quantum Gravity* (Springer, Berlin, 2020).

[25] E. Witten, *Riv. Nuovo Cim.* **43**, 187 (2020), arXiv:1805.11965 [hep-th].

[26] E. Witten, *Eur. Phys. J. Plus* **140**, 430 (2025), arXiv:2412.16795 [hep-th].

[27] J. Caminiti, F. Capeccia, L. Ciambelli, and R. C. Myers, *JHEP* **2025** (8), 166, arXiv:2502.02633 [hep-th].

[28] D. Tong, Quantum field theory, Lecture notes, University of Cambridge (2006–2012), see section 2.3 “The Vacuum” for discussion of $\delta(0)$ as volume.

[29] M. E. Peskin and D. V. Schroeder, *An Introduction to quantum field theory* (Addison-Wesley, Reading, USA, 1995).

[30] M. Srednicki, *Quantum field theory* (Cambridge University Press, 2007).

[31] S. Weinberg, *The Quantum theory of fields. Vol. 1: Foundations* (Cambridge University Press, 2005).

[32] C. Rovelli and M. Smerlak, *Phys. Rev. D* **85**, 124055 (2012).